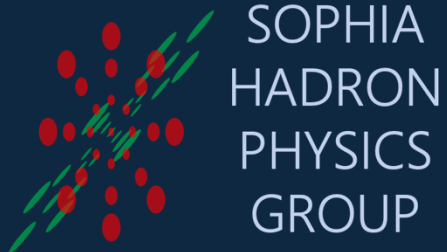


Rapidity scan in high-energy heavy-ion collisions

Shin-ei Fujii¹, Yasuki Tachibana², Tetsufumi Hirano¹

Sophia University¹, Akita International University²



Introduction

Model

Results

Summary and Outlook

High baryon number density at LHC energies

Nuclear compression + CGC

Ming Li, Ph.D thesis, U. of Minesota (2018)

M. Li and J. I. Kapusta, Phys. Rev. C **99**, 014906 (2019)

- Solving classical gluon fields of receding nuclear remnants
 ⇒ Rapidity loss Δy of nucleons

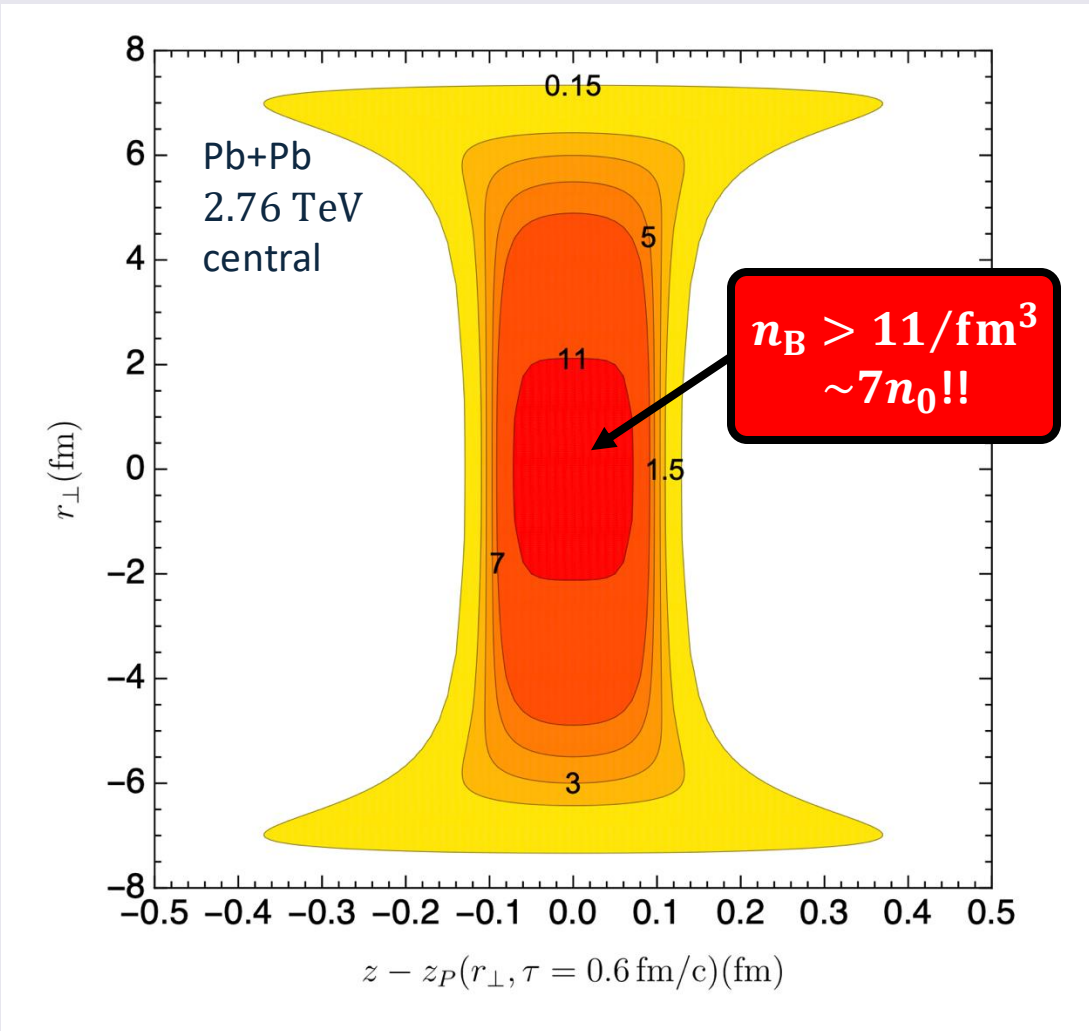
- Nuclear compression by Δy

$$n_B(x, y, z) \approx e^{\Delta y} \rho_A(x, y, ze^{\Delta y}) \text{ @high energy}$$

M. Gyulassy and L. P. Csernai, Nucl. Phys. A **460**, 723 (1986)

➔ **Extremely high baryon number density in the fragmentation regions of high-energy heavy ion collisions**


Baryon number density of compressed Pb



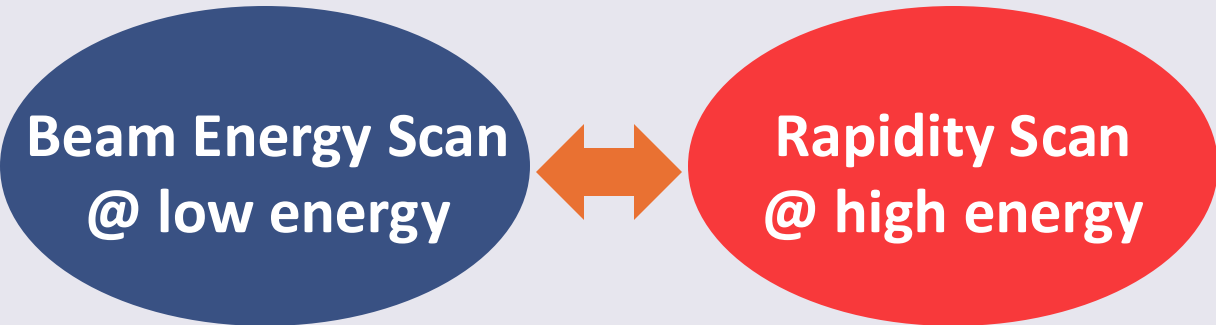
Rapidity Scan

Expected high baryon number density in forward rapidity in high-energy collisions

M. Li and J. I. Kapusta, Phys. Rev. C **99**, 014906 (2019)

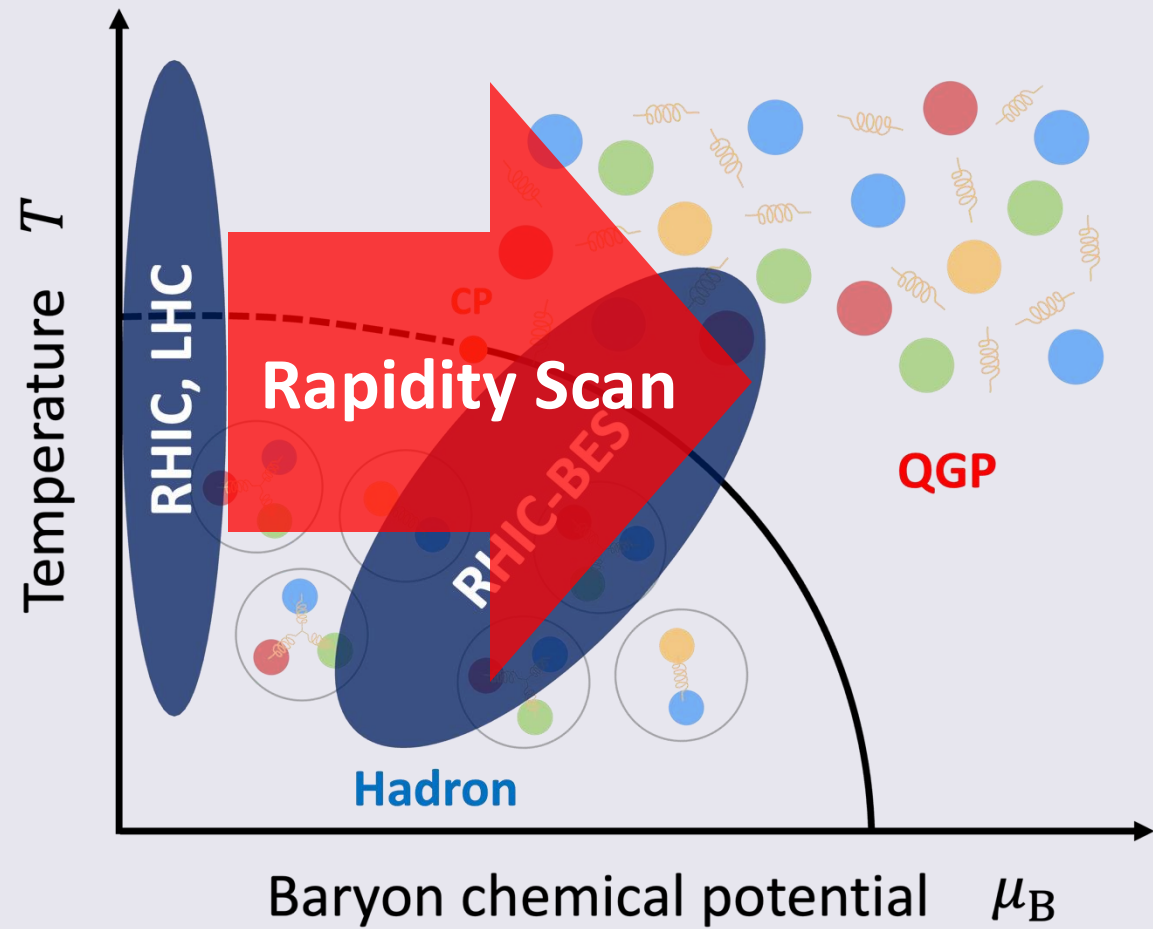

Rapidity Scan

Access high baryon chemical potential region in the QCD phase diagram



Complementary study of QCD phase diagram
by BES and Rapidity Scan!

QCD phase diagram and experiments



A fundamental question

How large baryon chemical potential is achieved as equilibrated matter in forward rapidity?

To answer the question, models must describe...

- Equilibrium and non-equilibrium components separately
- Fluidization (equilibration) of baryon number
- Hydrodynamic evolution of baryon number density

➔ **DCCI + finite n_B extension**

Introduction

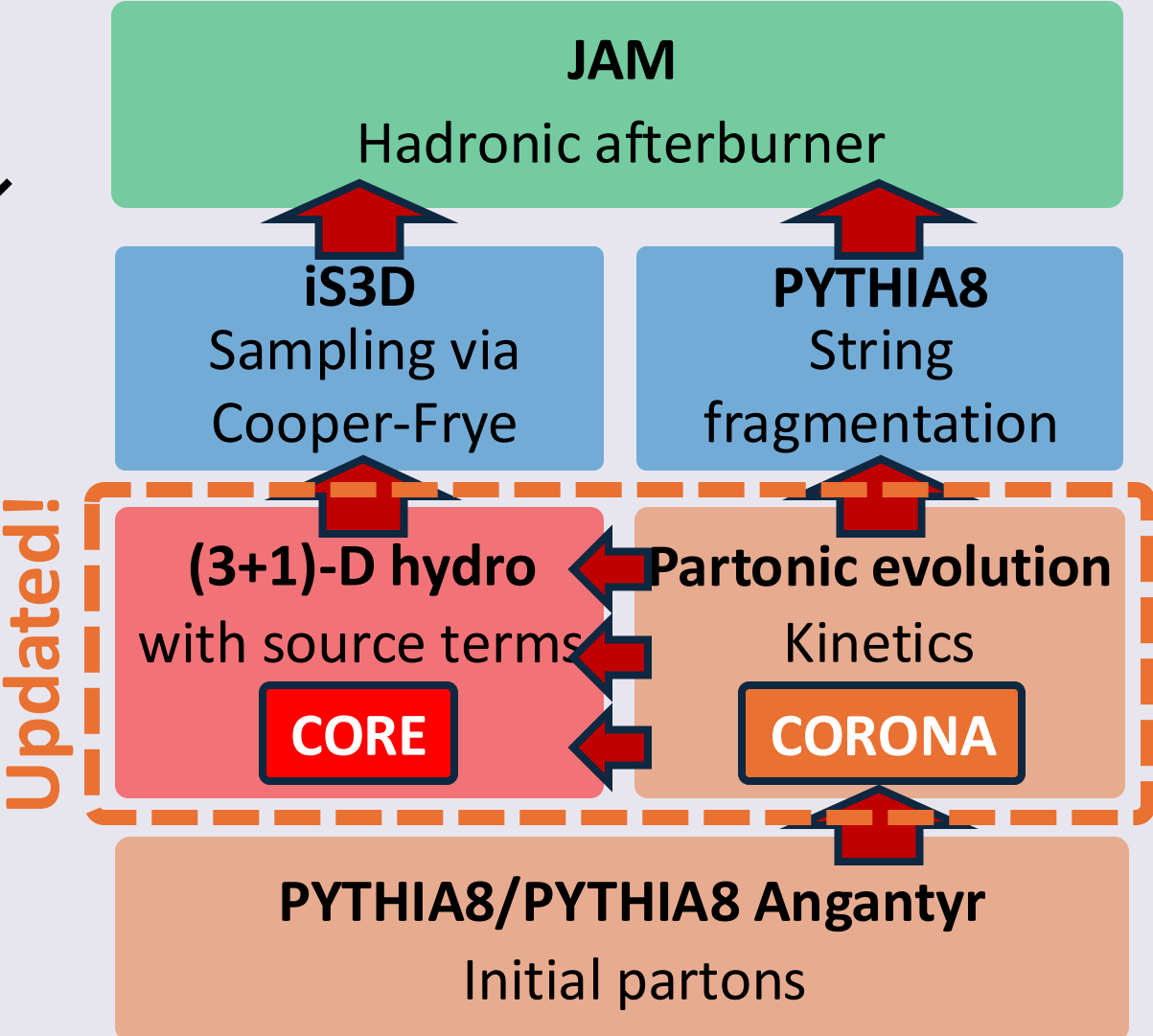
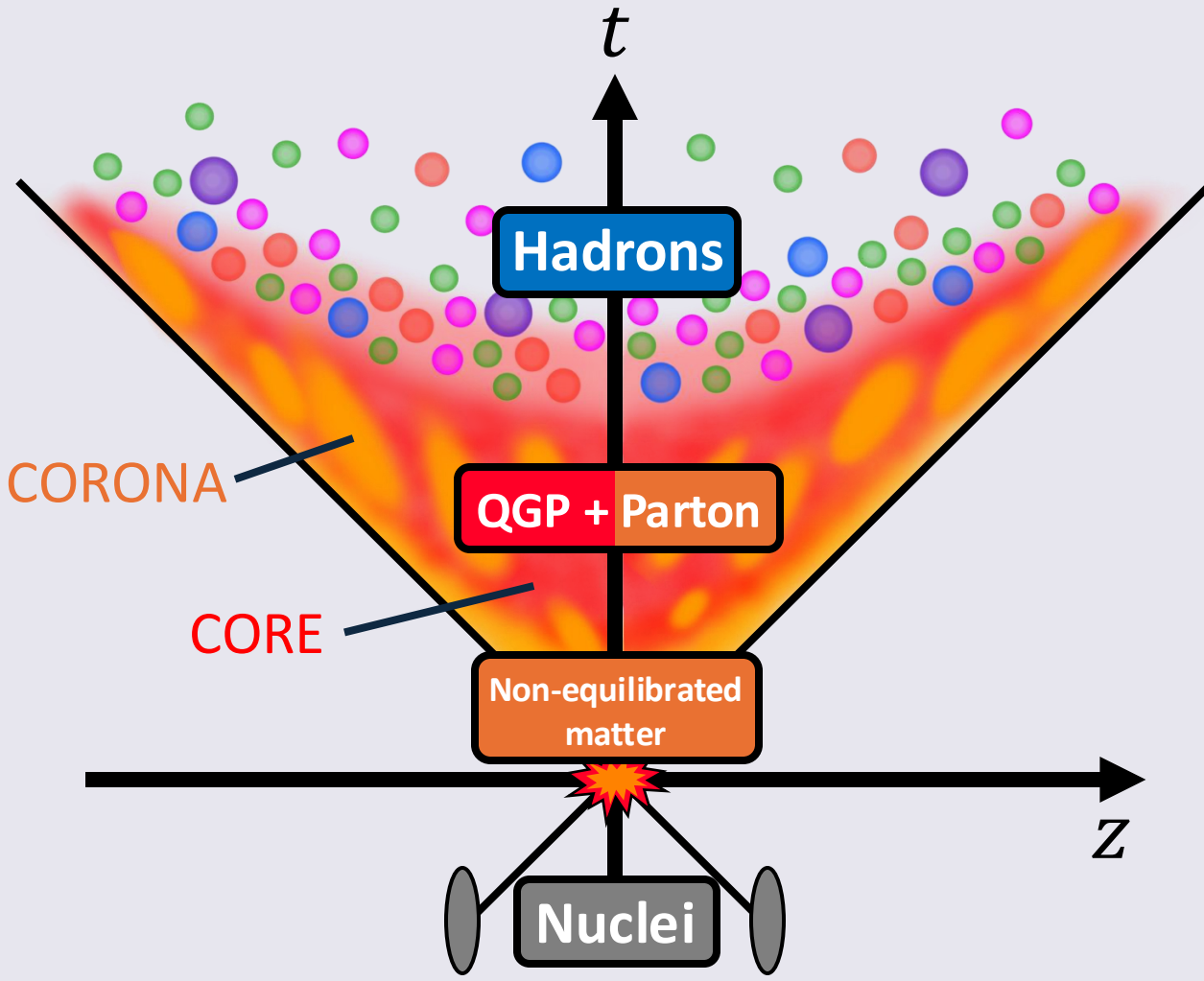
 **Model**

Results

Summary and Outlook

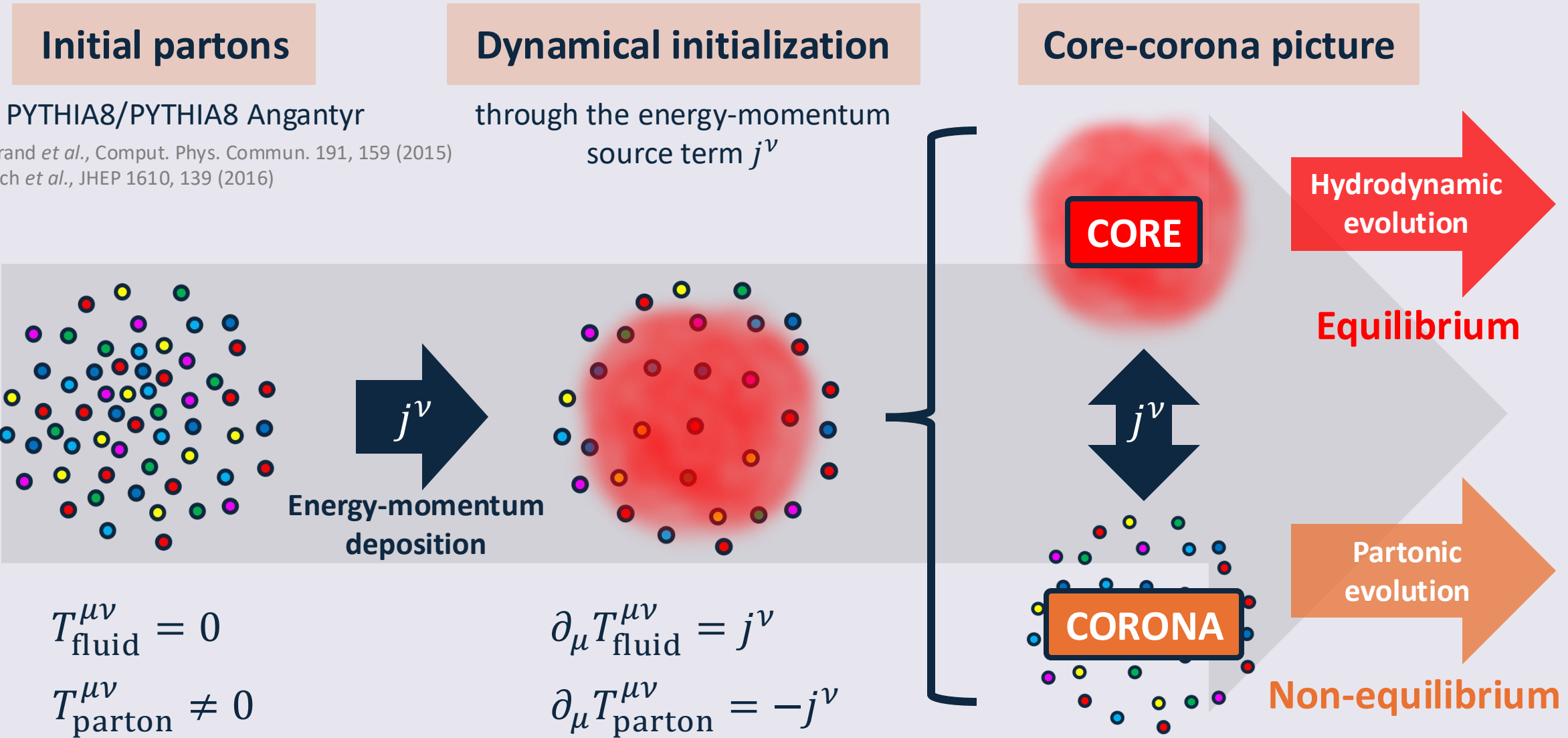
Dynamical Core-Corona Initialization (DCCI) model

Y. Kanakubo *et al.*, Phys. Rev. C **105**, 024905 (2022)



Dynamical Core-Corona Initialization (DCCI) model

Y. Kanakubo *et al.*, Phys. Rev. C **105**, 024905 (2022)



Hydrodynamic module in DCCI

Continuity eq. for entire system

$$\partial_\mu (T_{\text{fluid}}^{\mu\nu} + T_{\text{parton}}^{\mu\nu}) = 0$$

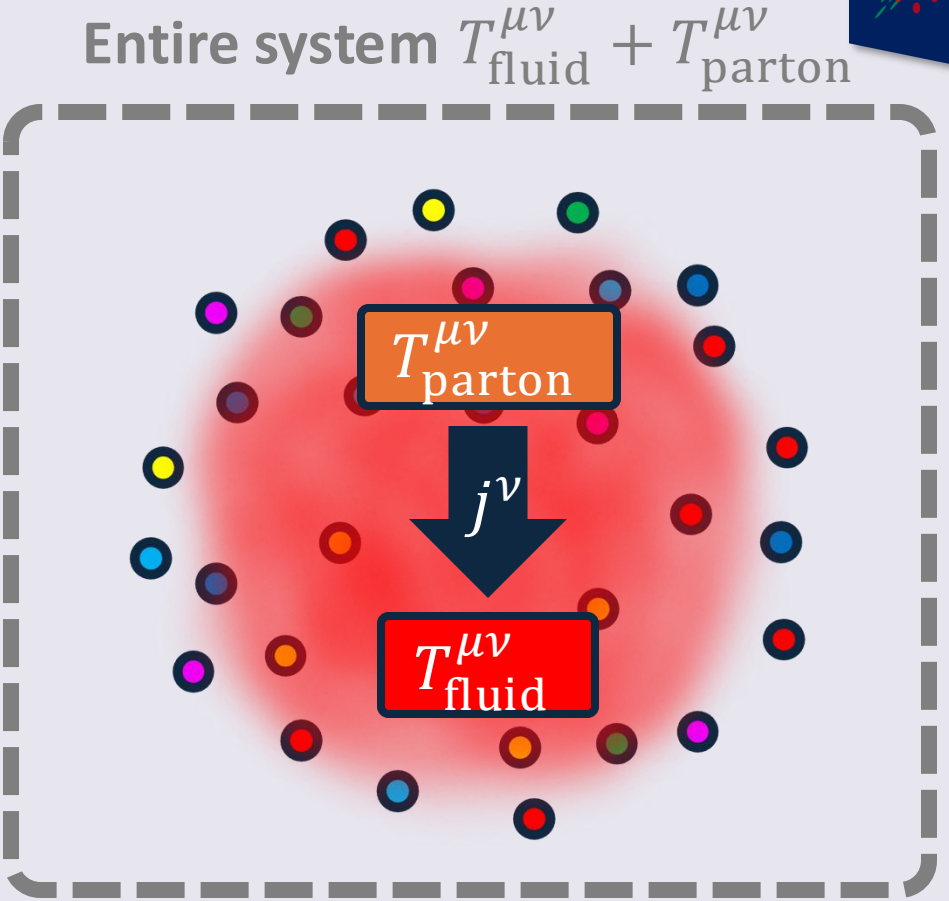
Hydrodynamic eqs. with E-M source term

$$\partial_\mu T_{\text{fluid}}^{\mu\nu} = j^\nu \quad j^\nu = -\partial_\mu T_{\text{parton}}^{\mu\nu}$$

Fluidization rate

$$j^\nu = - \sum_i^{N_{\text{parton}}} \left[\frac{dp_i^\nu(t)}{dt} \right] G(\mathbf{x} - \mathbf{x}_i(t))$$

p_i^ν : Four-momentum of i_{th} parton
 G : Gaussian function \mathbf{x}_i : Position of i_{th} parton



Assumptions

- Straight trajectory of partons
- Instant equilibration of deposited E-M
- Gaussian profile

Energy-momentum source term

Phenomenological fluidization rate per particle in core-corona picture

$$\frac{dp_i^\mu}{d\tau} = - \sum_j^{N_{\text{scat}}} \rho_{i,j} \sigma_{i,j} |v_{\text{rel},i,j}| p_i^\mu$$

$\rho_{i,j}$: Effective density of j_{th} seen from i_{th}
 $\sigma_{i,j}$: Cross section between i_{th} and j_{th}
 $v_{\text{rel},i,j}$: Relative velocity between i_{th} and j_{th}

● Collision detection

$$b_{i,j} \leq \sqrt{\frac{\sigma_{i,j}}{\pi}}$$

Low p_T / Dense region → CORE (QGP)

High p_T / Dilute region → CORONA (Partons)

● Cross section

$$\sigma_{i,j} = \min \left\{ \frac{\sigma_0}{s_{i,j}}, \pi b_{\text{cut}}^2 \right\}$$

$\sigma_0 = 0.3 \text{ fm}^2$ $b_{\text{cut}} = 1.0 \text{ fm}$

Event by event initial condition for QGP fluid

Extension to finite charges

Extension to finite charges

Hydrodynamic eqs. with source terms

$$\partial_\mu N_{\text{fluid}, I}^\mu = \rho_I \quad I: B, Q, S$$

When i_{th} parton deposits all energy
= dead parton

Source terms of conserved charges

$$\rho_I = - \sum_j^{N_{\text{dead}}} \frac{dN_{j,I}}{dt} G(\mathbf{x} - \mathbf{x}_j(t))$$

$N_{j,I}$: Charge I of j_{th} dead parton
 G : Gaussian function \mathbf{x}_j : Position of j_{th} dead parton

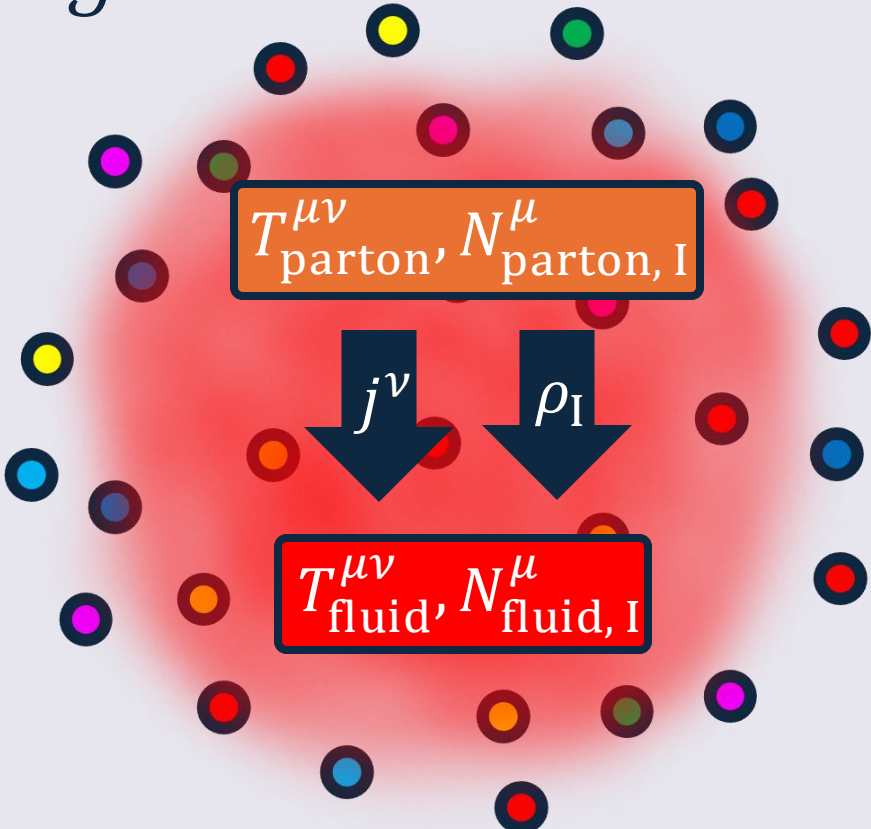
Fluidization (equilibration) and Hydrodynamic evolution of conserved charges (B, Q, S)

Summary of hydrodynamic equations

$$\partial_\mu T^{\mu\nu} = j^\nu$$

$$T^{\mu\nu} = (e + P)u^\mu u^\nu - P g^{\mu\nu}$$

$\partial_\mu N_B^\mu = \rho_B$	$N_B^\mu = n_B u^\mu$	Updated!
$\partial_\mu N_Q^\mu = \rho_Q$	$N_Q^\mu = n_Q u^\mu$	
$\partial_\mu N_S^\mu = \rho_S$	$N_S^\mu = n_S u^\mu$	



- Ideal hydrodynamics with source terms
- 7 independent variables
- Equation of state with d.o.f (e, n_B, n_Q, n_S) is needed

NEOS-4D

● Taylor expansion using Lattice results (high T)

$$\frac{P}{T^4} = \frac{P_0}{T^4} + \sum_{l,m,n} \frac{x_{l,m,n}^{B,Q,S}}{l! m! n!} \left(\frac{\mu_B}{T}\right)^l \left(\frac{\mu_Q}{T}\right)^m \left(\frac{\mu_S}{T}\right)^n$$

● Hadron gas (low T)

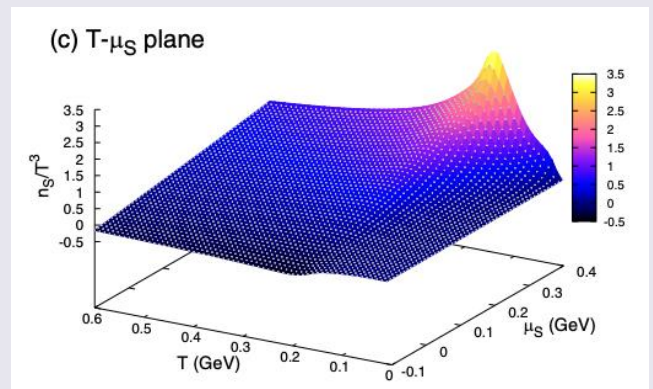
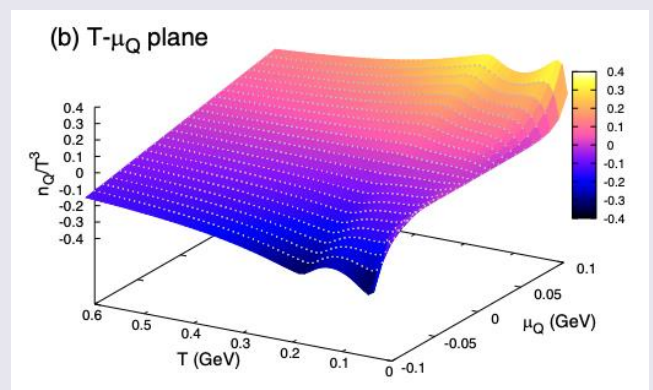
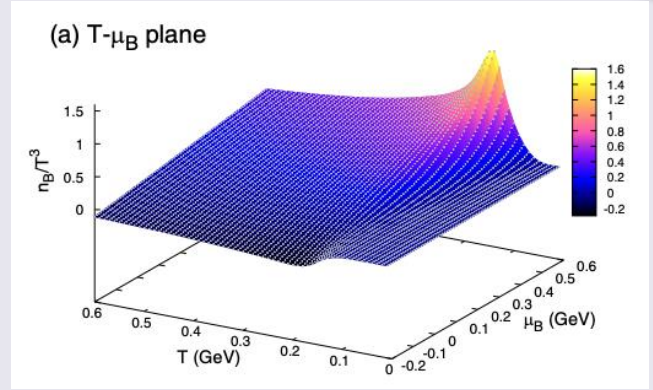
$$P = \pm T \sum_i \int \frac{g_i d^3p}{(2\pi)^3} \ln[1 \pm e^{-(E_i - \mu_i)/T}]$$

CONNECT

$$\frac{P}{T^4} = \frac{1}{2} \left[1 - \tanh \frac{T - T_c}{\Delta T_c} \right] \frac{P_{\text{had}}}{T^4} + \frac{1}{2} \left[1 + \tanh \frac{T - T_c}{\Delta T_c} \right] \frac{P_{\text{lat}}}{T^4}$$

NEOS-2D: $n_Q = 0.4n_B, n_S = 0$

NEOS-4D: No constraint



Introduction

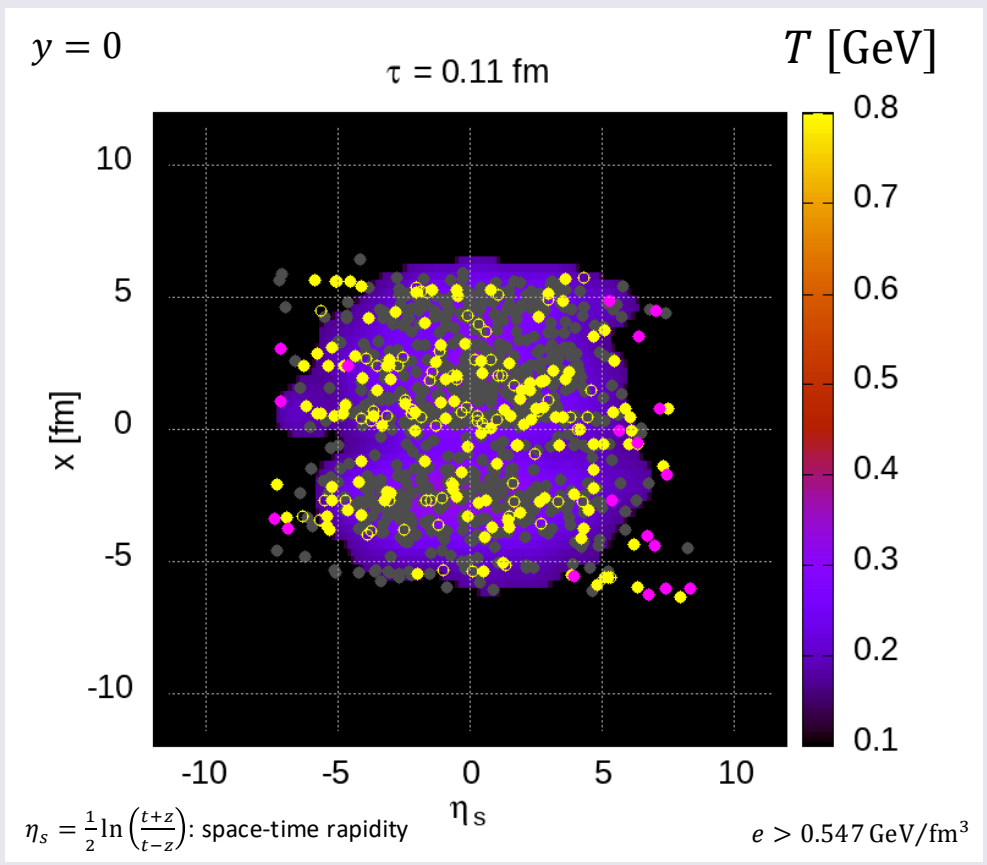
Model

 **Results**

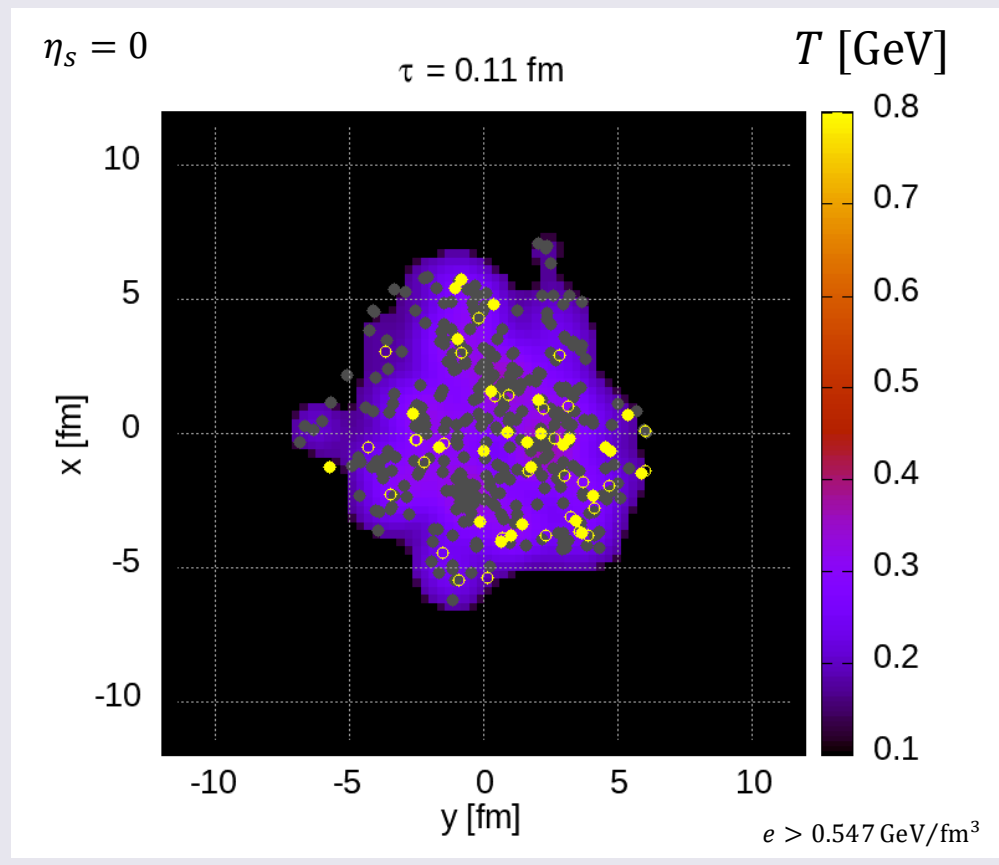
Summary and Outlook

Evolution of core and corona

Temperature (longitudinal profile)



Temperature (transverse profile)



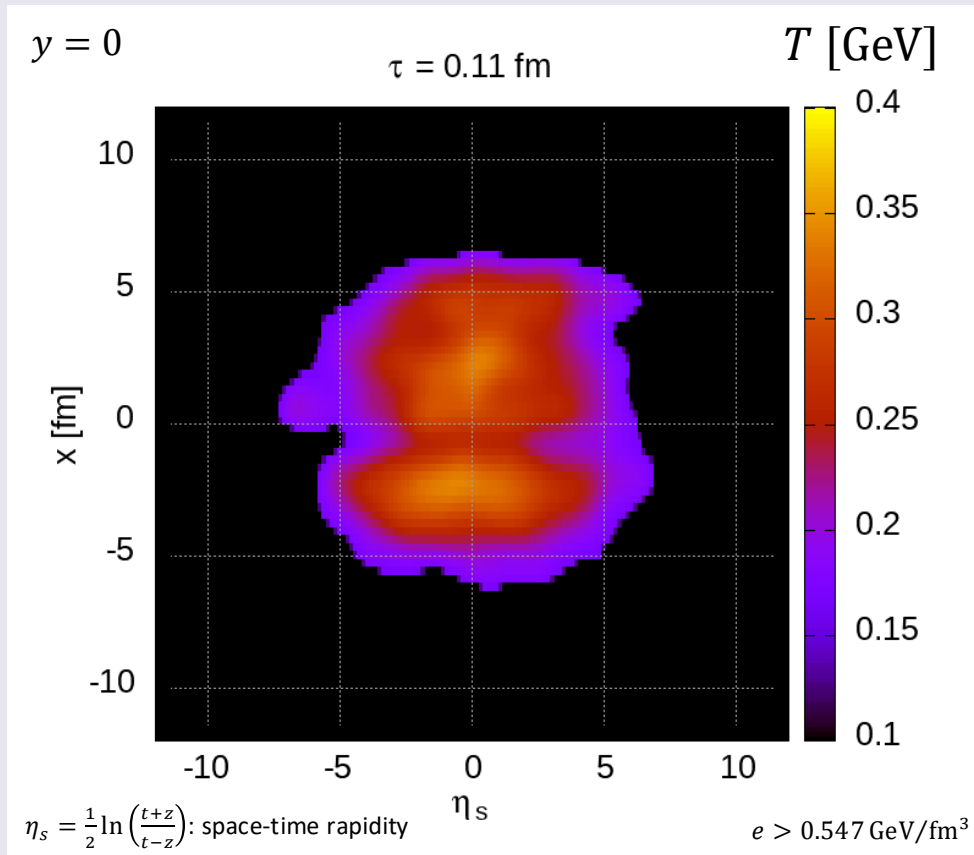
- : quark
- : anti-quark
- : diquark
- : anti-diquark
- : gluon

$\tau = 0.1 - 0.3$ fm: $\Delta\tau = 0.01$ fm → Fluid formation

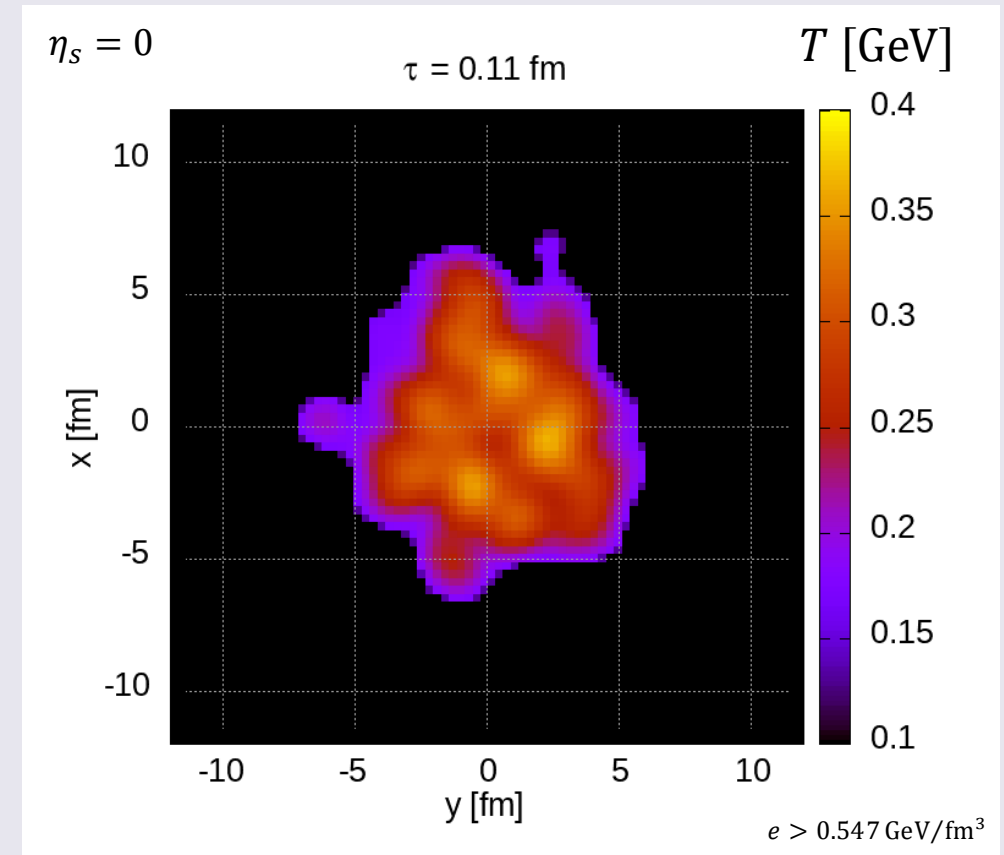
$\tau > 0.3$ fm: $\Delta\tau = 0.3$ fm → Fluid evolution

Temperature

Temperature (longitudinal profile)



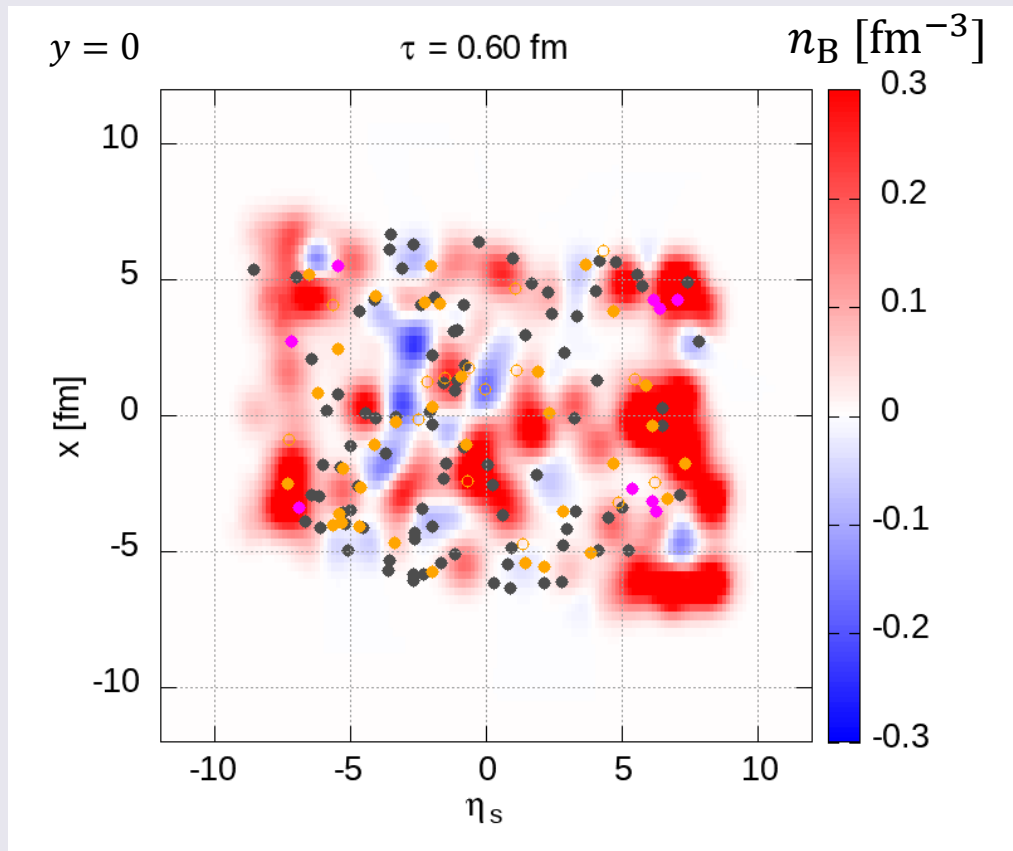
Temperature (transverse profile)



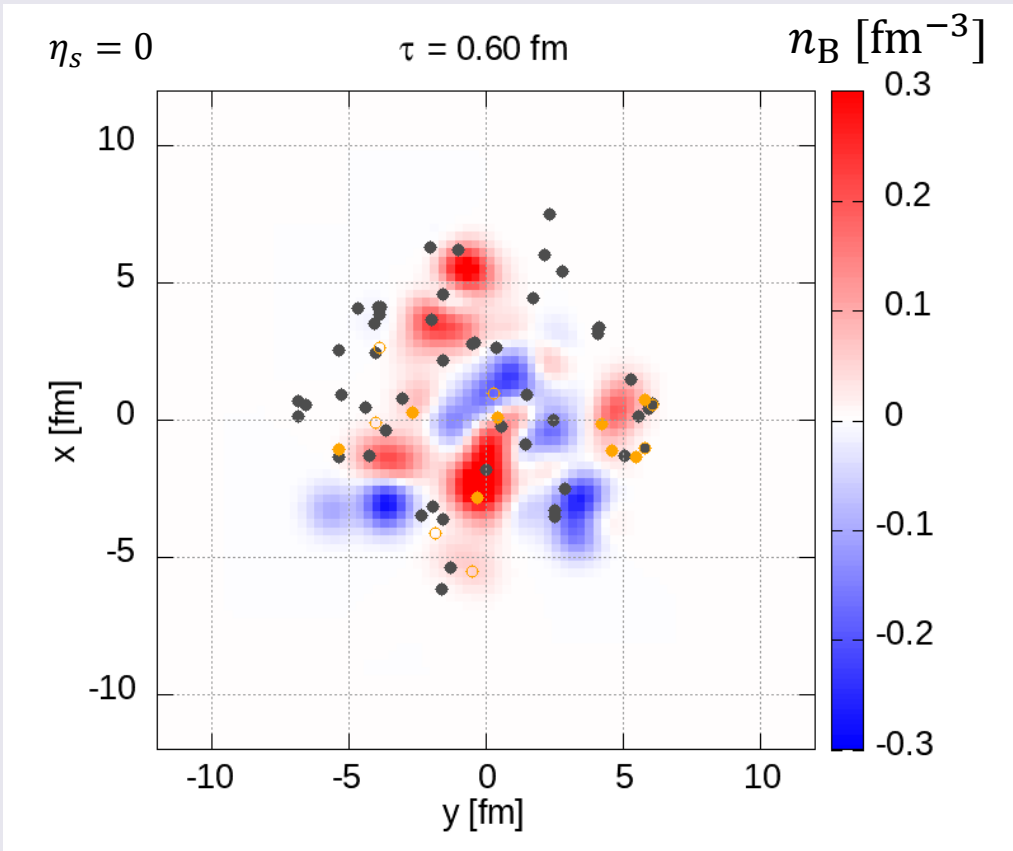
- Gradual formation of the core (QGP fluid) through the energy-momentum source term
- Alongside the fluid formation, the core cools down due to the hydrodynamic evolution

Evolution of core and corona

Baryon number density (longitudinal profile)



Baryon number density (transverse profile)

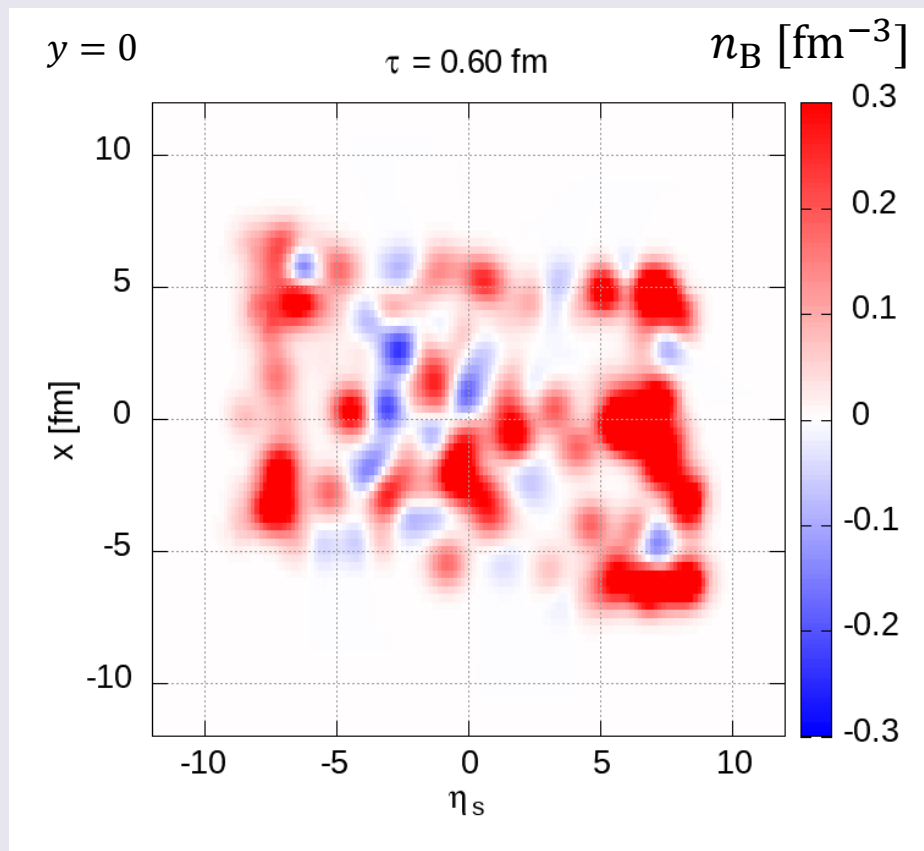


- : quark ● : diquark ● : gluon
- : anti-quark ○ : anti-diquark

$\tau > 0.3$ fm: $\Delta\tau = 0.3$ fm \rightarrow Fluidization of baryon number

Baryon number density

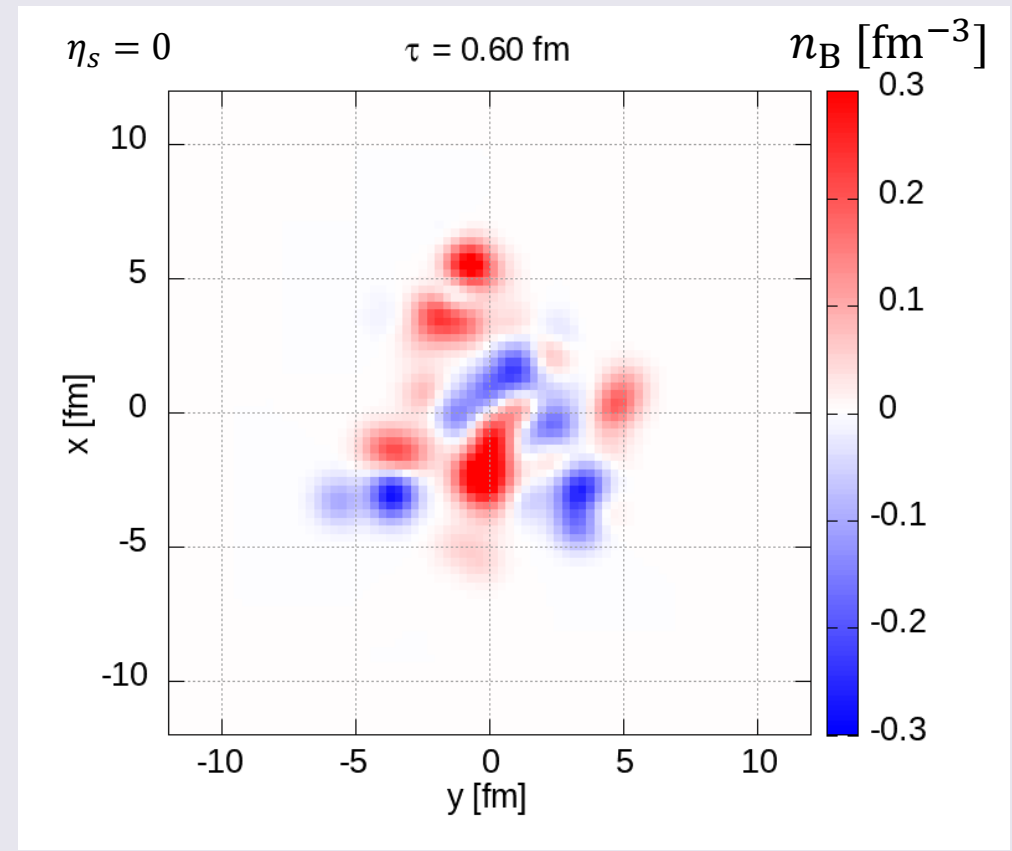
Baryon number density (longitudinal profile)



- Large equilibrated baryon number density in forward rapidities $5 \lesssim |\eta_s| \lesssim 10$

cf.) $y_{\text{beam}}(\sqrt{s_{\text{NN}}} = 2.76 \text{ TeV}) \approx 8$

Baryon number density (transverse profile)

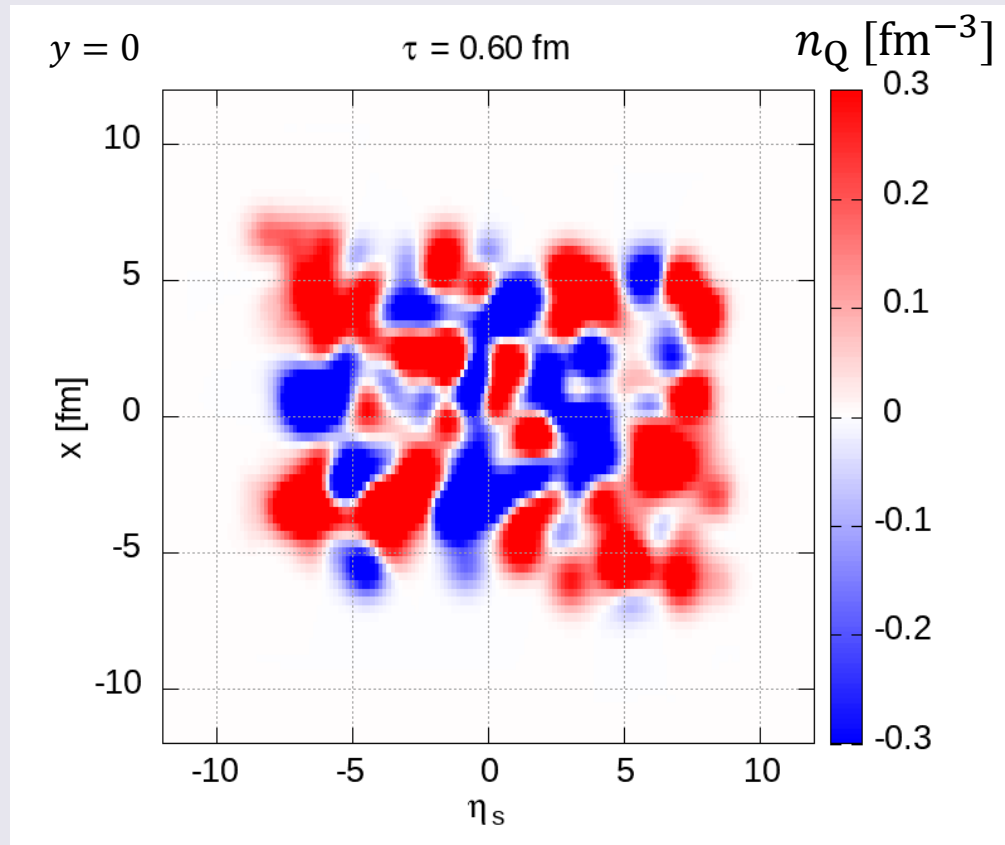


- Large fluctuations of baryon number density even in midrapidity

➡ Negative n_B region appears

Electric charge density

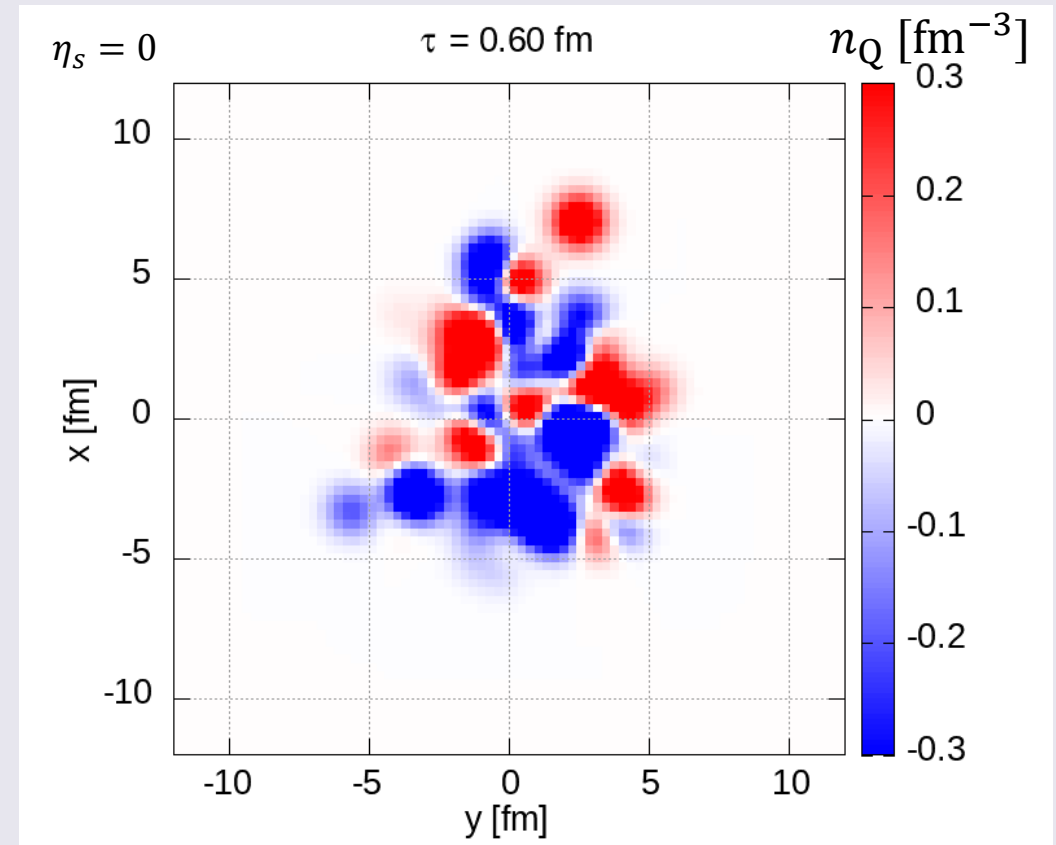
Electric charge density (longitudinal profile)



- Large equilibrated electric charge density in forward rapidities $5 \lesssim |\eta_s| \lesssim 10$

cf.) $n_Q \approx 0.4n_B$ (Pb)

Electric charge density (transverse profile)

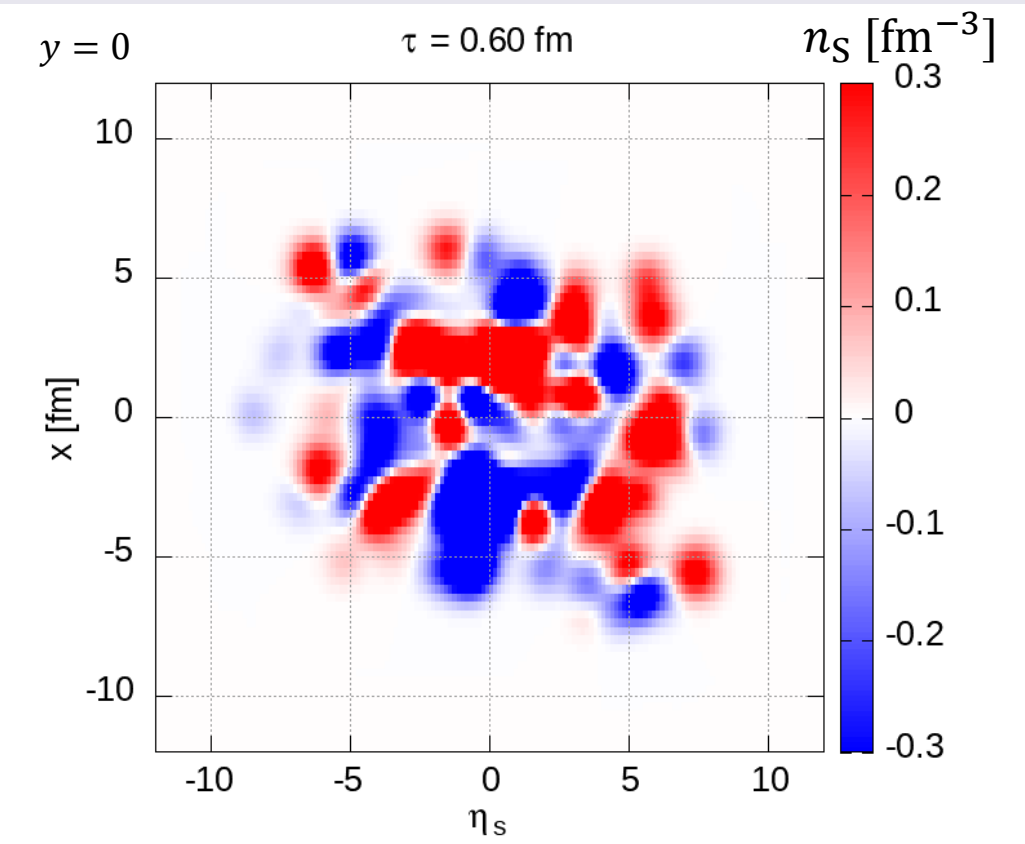


- Large fluctuations of electric charge density even in midrapidity

➔ Negative n_Q region appears

Strangeness density

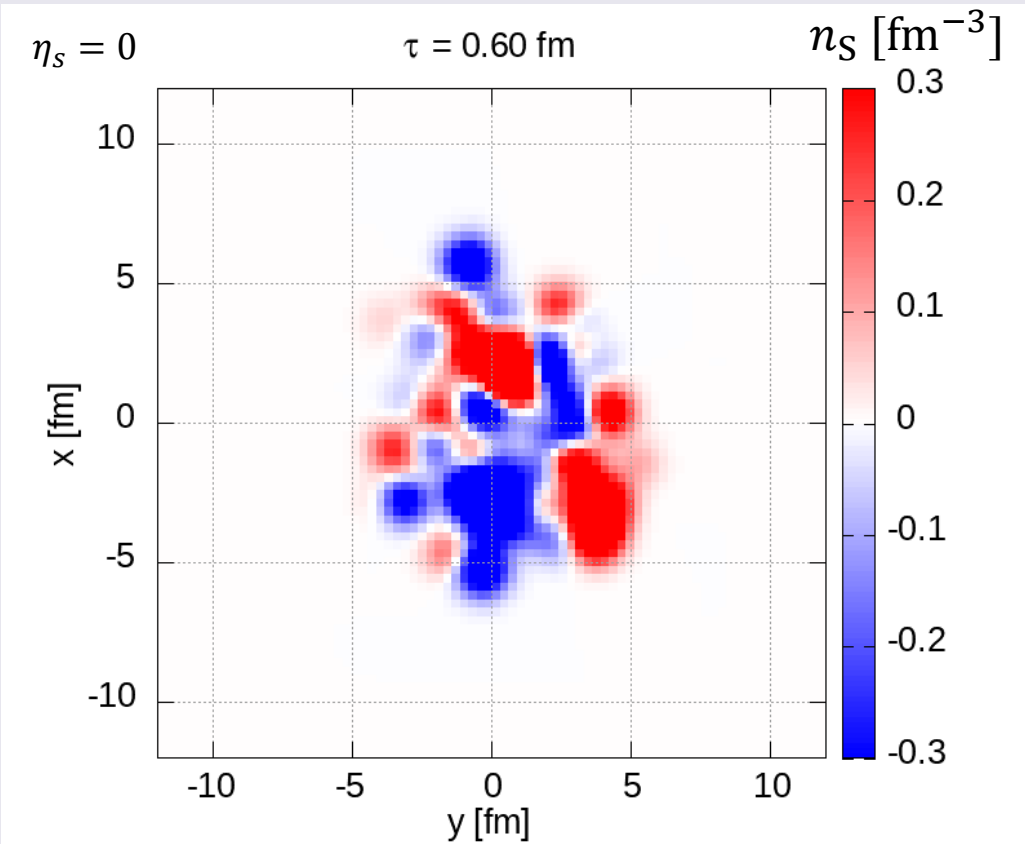
Strangeness density (longitudinal profile)



- No large strangeness density region in forward rapidity

cf.) $n_s = 0$ (Pb)

Strangeness density (transverse profile)



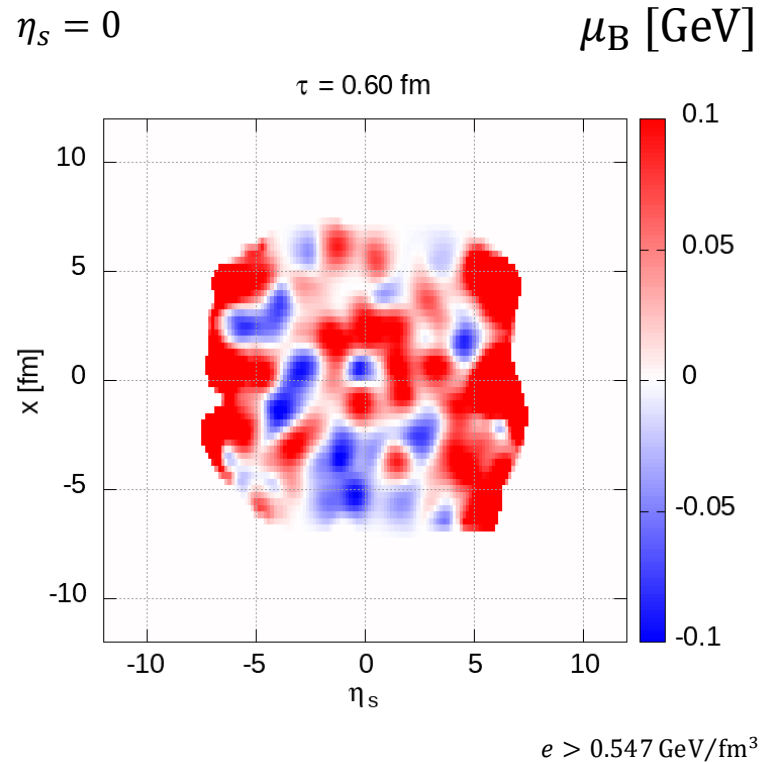
- Large fluctuations of strangeness density even in midrapidity

➔ Negative n_s region appears

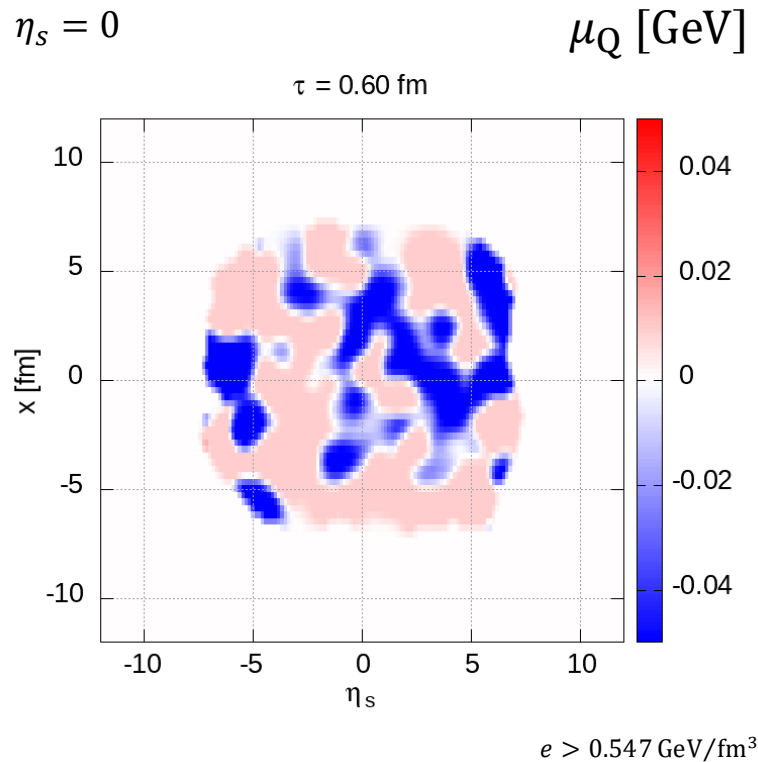
Chemical potentials (longitudinal)

Pb+Pb 2.76 TeV, $b = 2.46$ fm
Single event

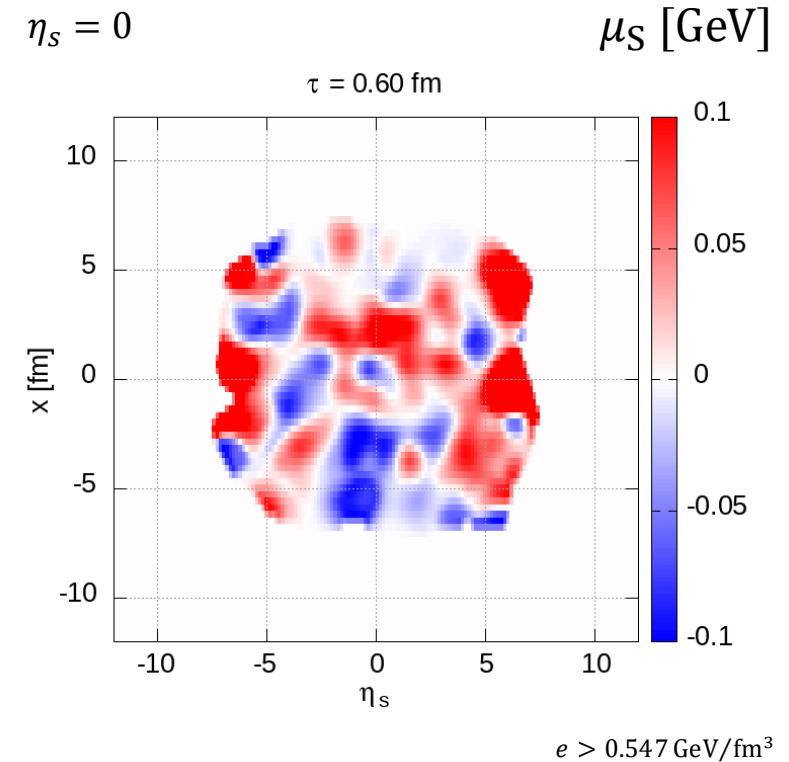
Baryon chemical potential



Electric charge chemical potential



Strangeness chemical potential



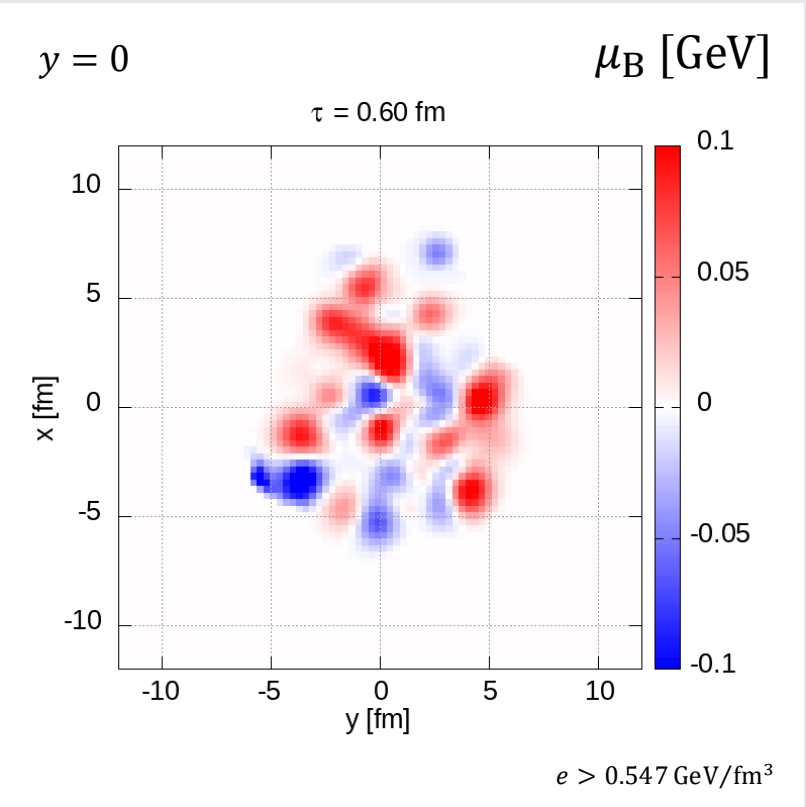
● High μ_B in forward rapidities

● Large negative μ_Q and small positive μ_Q

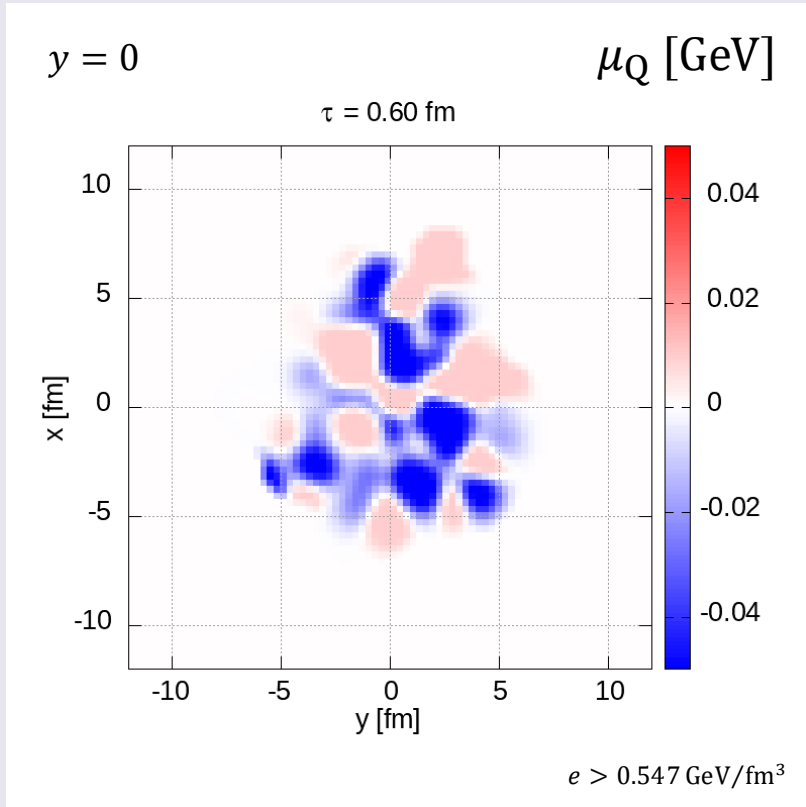
● Relatively high μ_S in forward rapidities

Chemical potentials (transverse)

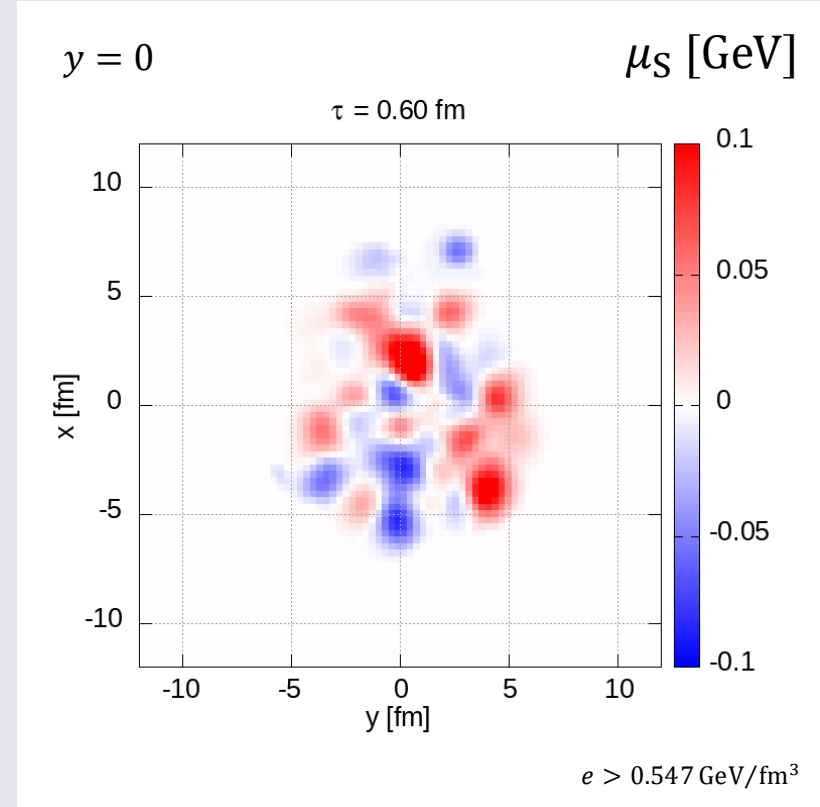
Baryon chemical potential



Electric charge chemical potential



Strangeness chemical potential



● Large fluctuations around zero chemical potential

● Large negative μ_Q and small positive μ_Q

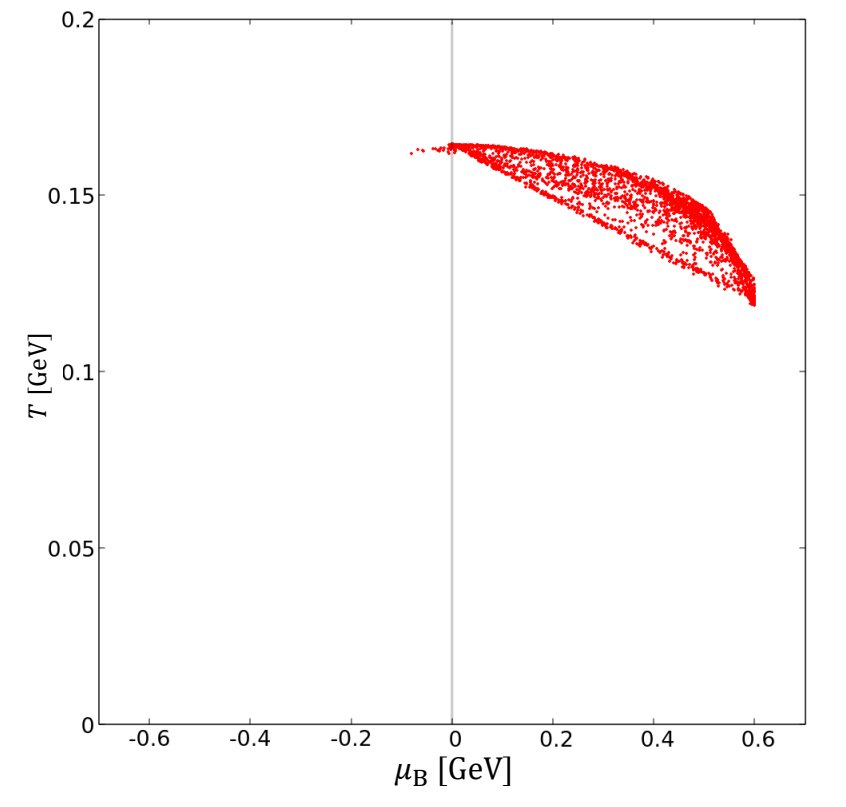
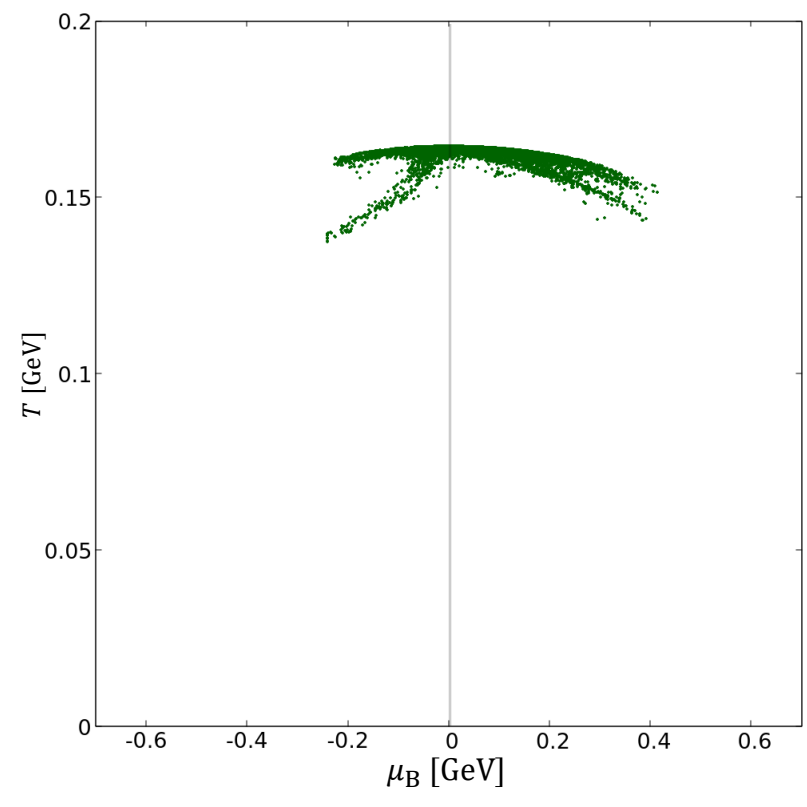
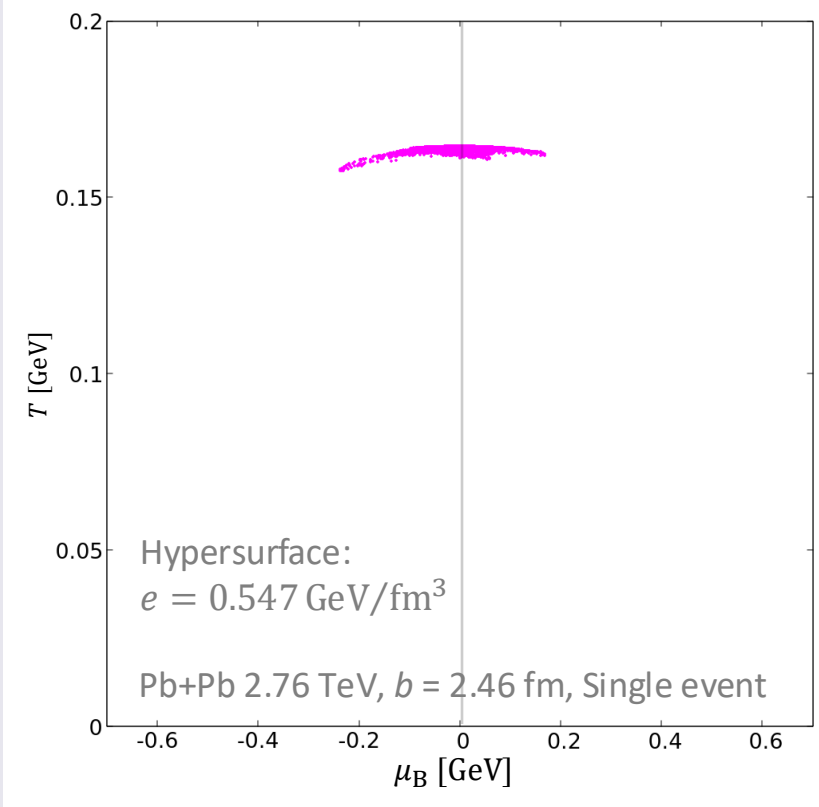
● Large fluctuations around zero chemical potential

Rapidity dependence of freezeout hypersurface (B)

$-1 \leq \eta_s \leq 1$

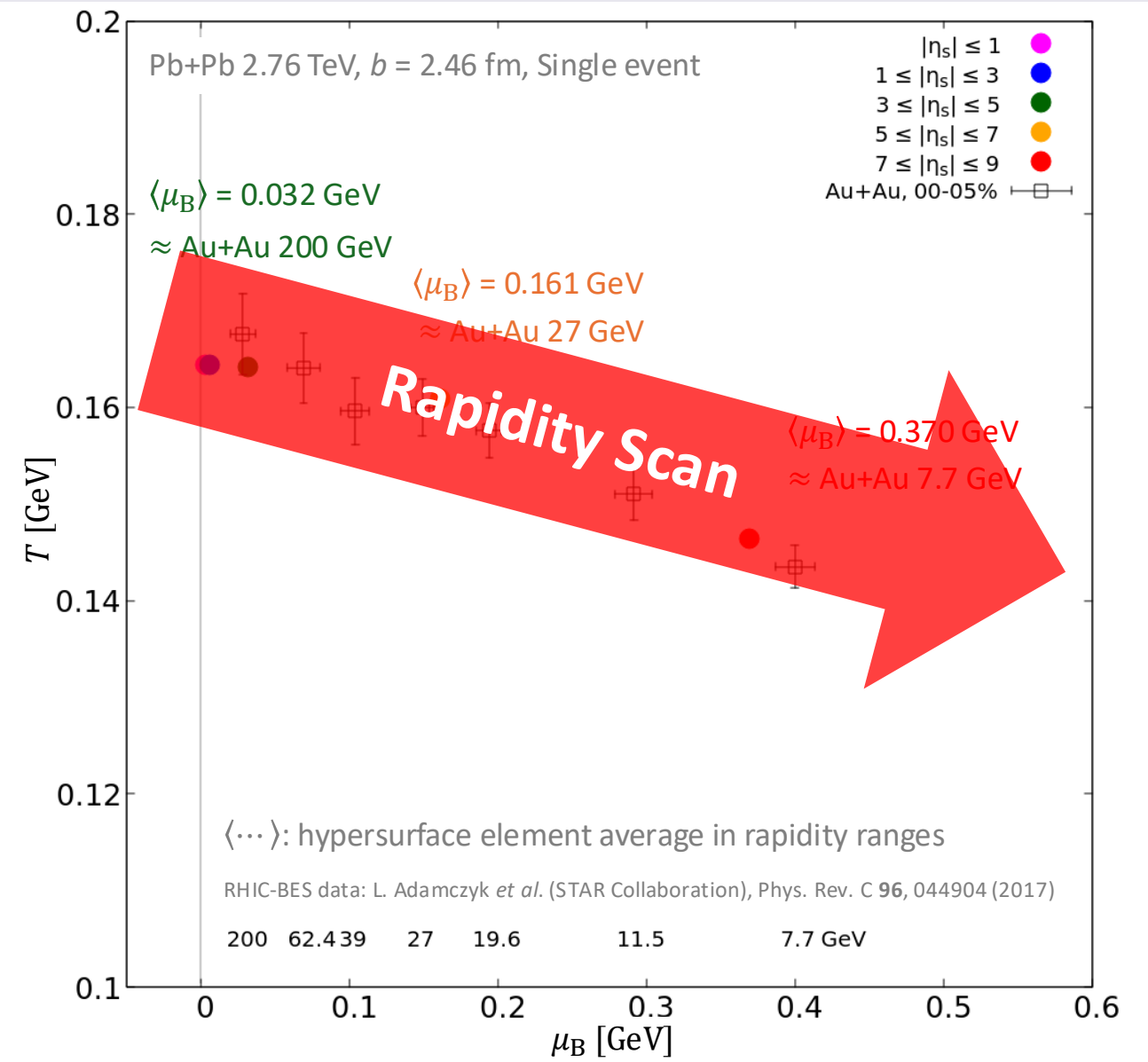
$3 \leq \eta_s \leq 5$

$7 \leq \eta_s \leq 9$



- Some hypersurface element has negative baryon chemical potentials
- Significantly large baryon chemical potentials in forward rapidities

Rapidity-averaged freezeout hypersurface (B)



- Almost zero baryon chemical potential until $|\eta_s| \leq 5$
 - $\Rightarrow \approx$ Au+Au 200 GeV
- Averaged-hypersurface in rapidity range $5 \leq |\eta_s| \leq 7$ exceeds $\mu_B = 100$ MeV
 - $\Rightarrow \approx$ Au+Au 27 GeV
- Averaged-hypersurface in rapidity range $7 \leq |\eta_s| \leq 9$ exceeds $\mu_B = 300$ MeV
 - $\Rightarrow \approx$ Au+Au 7.7 GeV

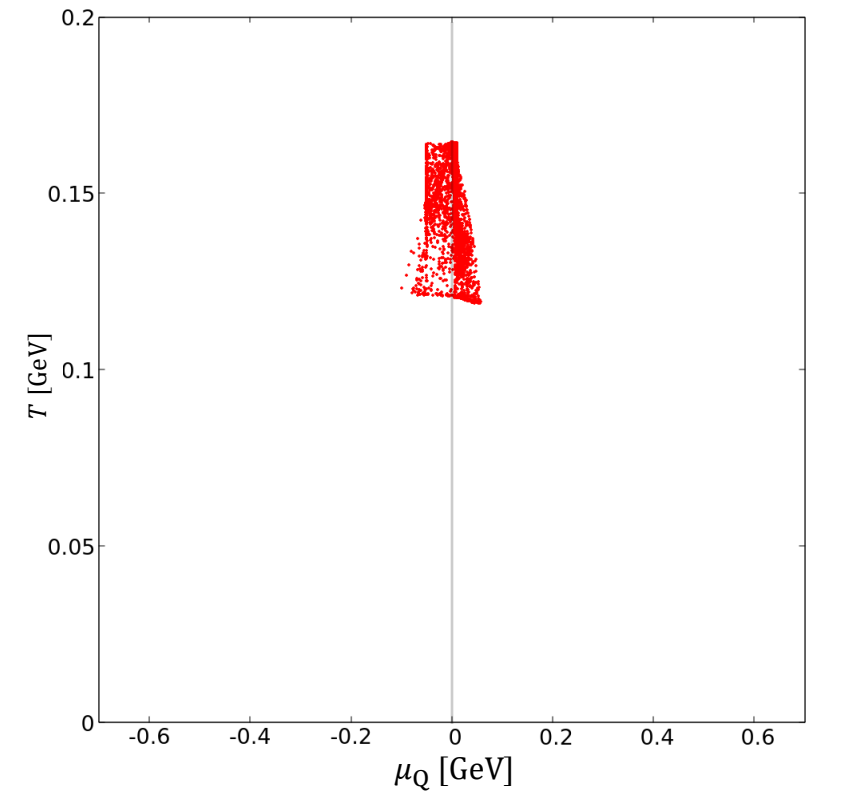
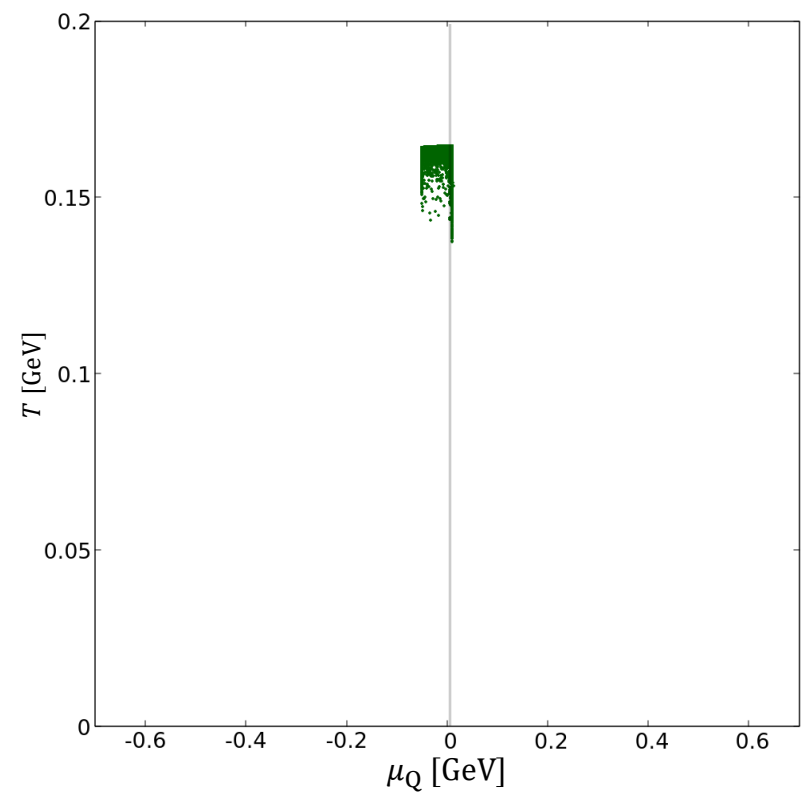
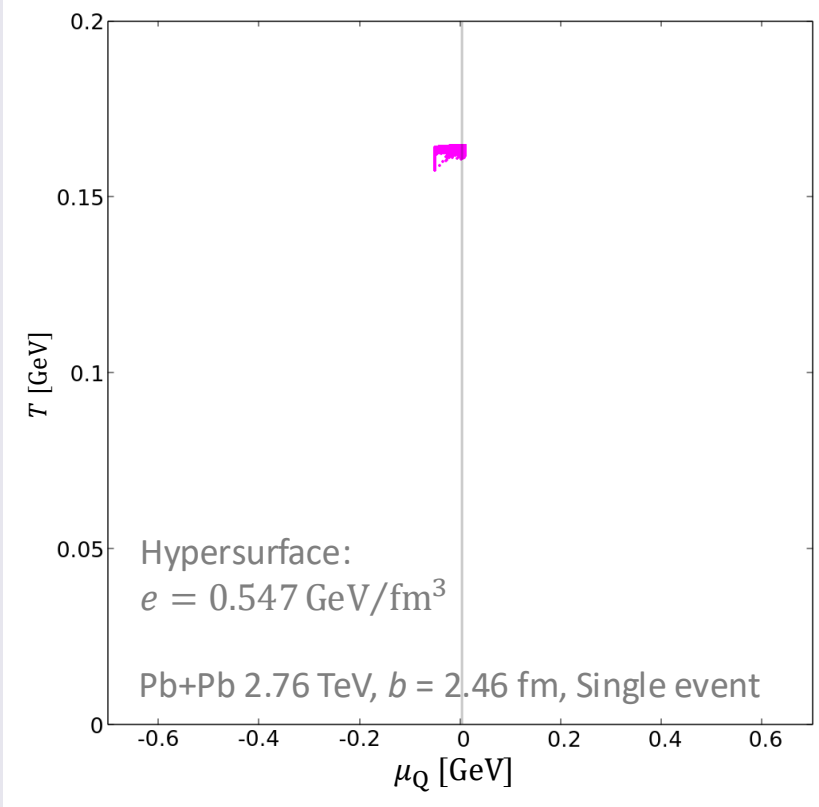
Rapidity scan is a strong tool for exploring the QCD phase diagram!!

Rapidity dependence of freezeout hypersurface (Q)

$-1 \leq \eta_s \leq 1$

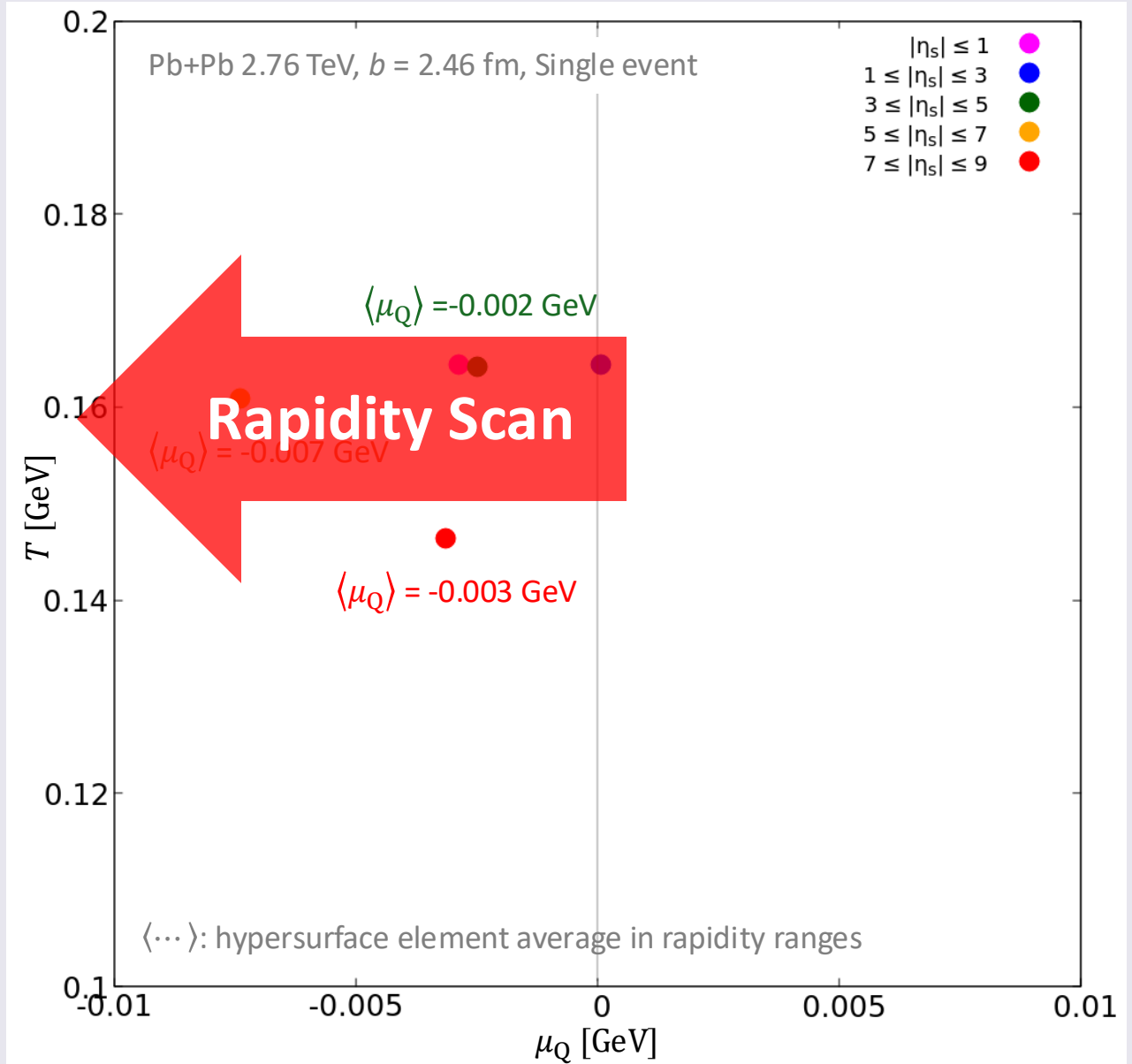
$3 \leq \eta_s \leq 5$

$7 \leq \eta_s \leq 9$



- Insufficient available range of NEOS-4D, $-0.05 < \mu_Q < 0.01$ GeV
- Tend to be negative chemical potentials in every rapidity range

Rapidity-averaged freezeout hypersurface (Q)



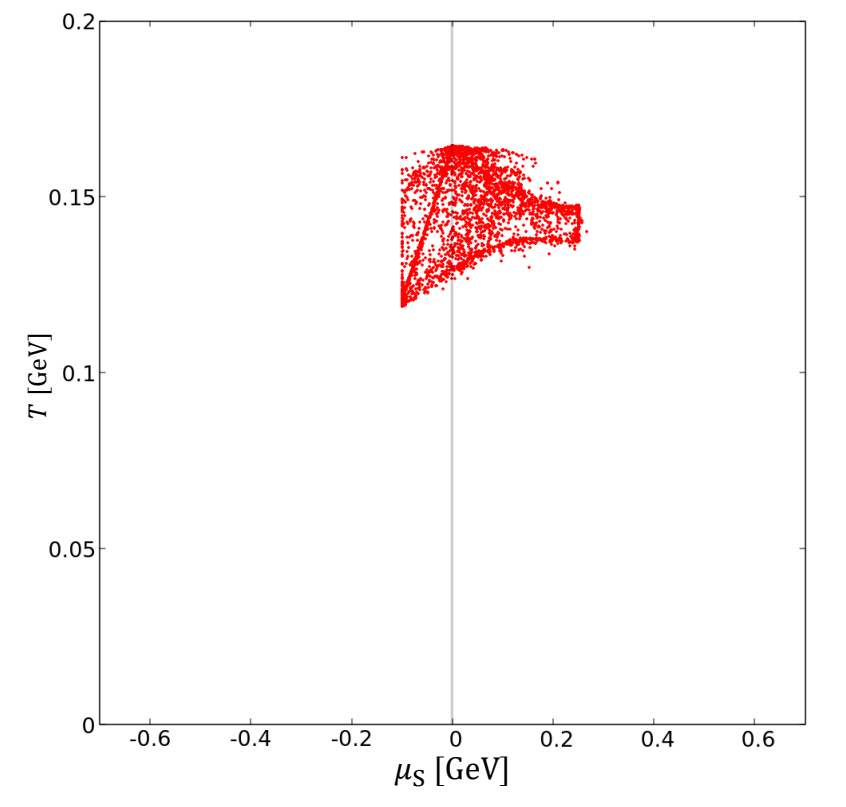
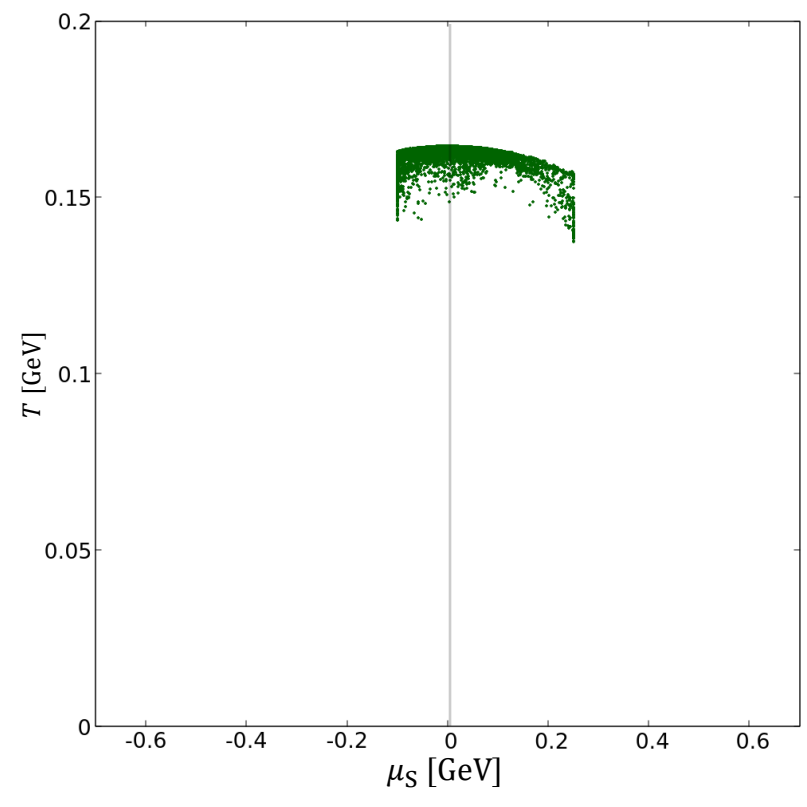
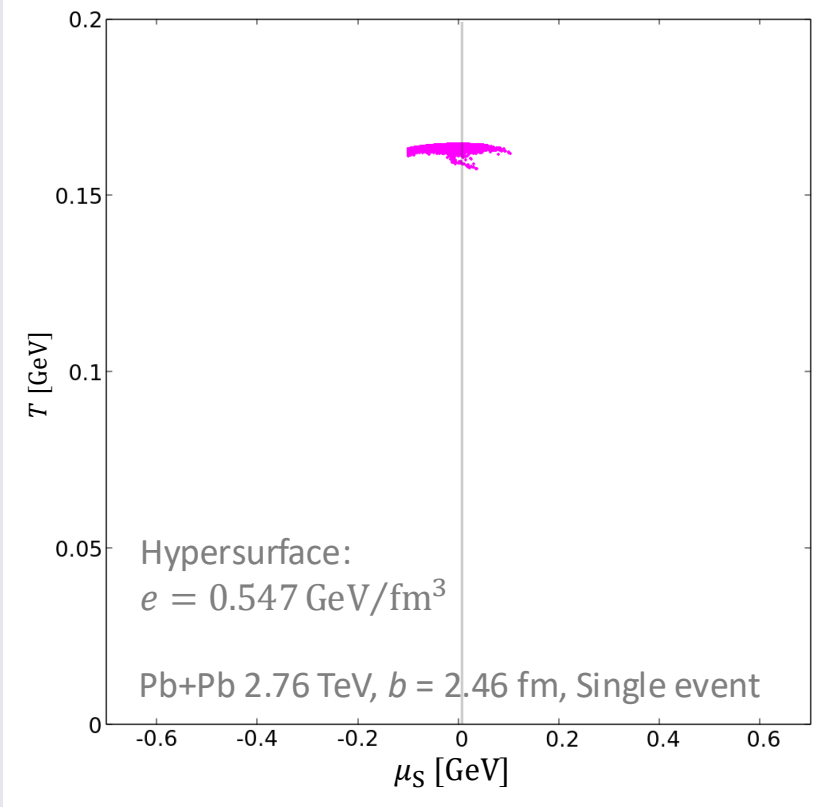
- Absolute value of electric charge chemical potentials are small
- Electric charge chemical potentials tend to be negative as go forward rapidity
- Need more statistics to make strict conclusions
- Need wider range EoS

Rapidity dependence of freezeout hypersurface (S)

$-1 \leq \eta_s \leq 1$

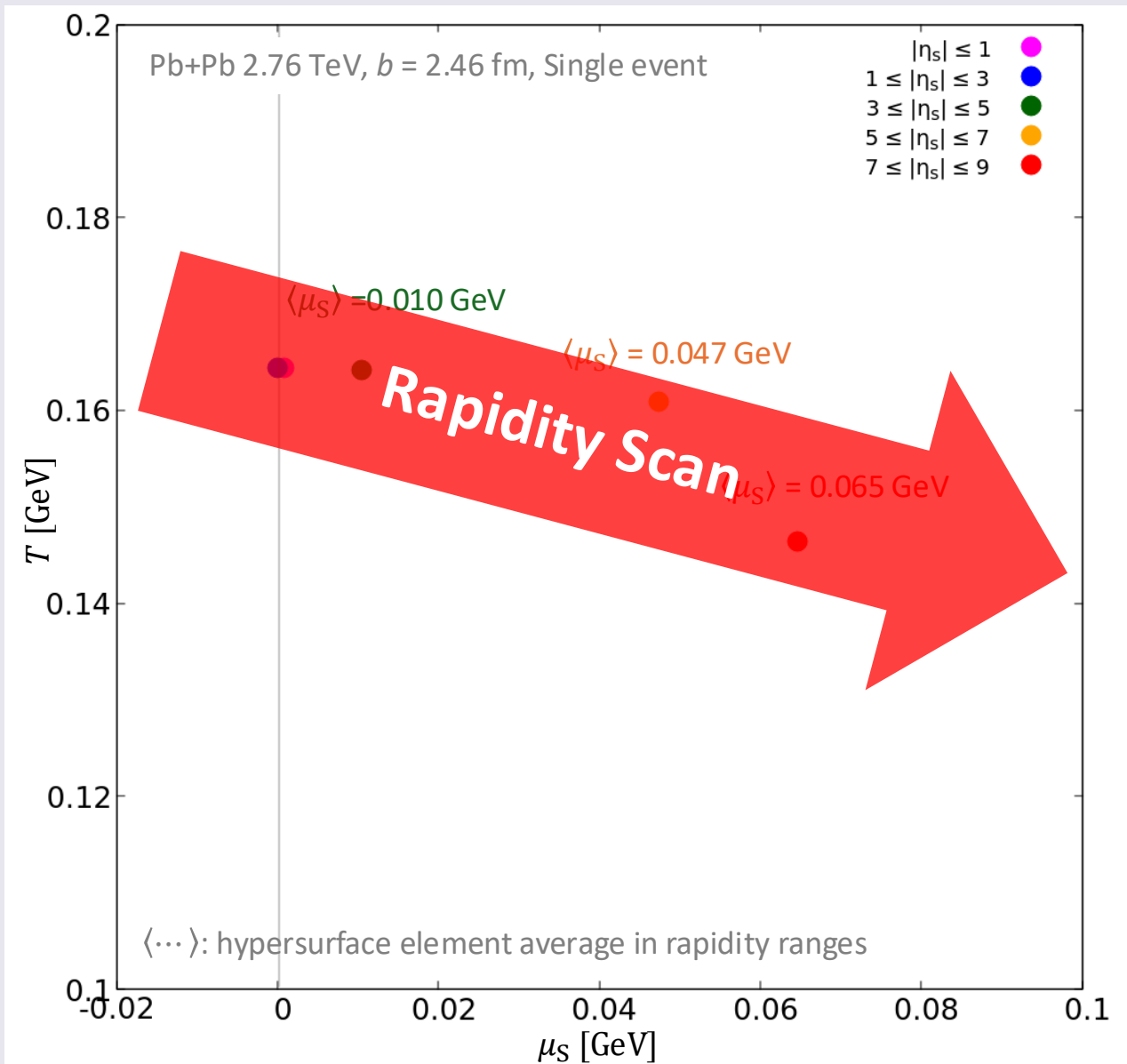
$3 \leq \eta_s \leq 5$

$7 \leq \eta_s \leq 9$



- Insufficient available range of NEOS-4D, $-0.1 < \mu_s < 0.25$ GeV
- Tend to be positive chemical potentials as go forward rapidity

Rapidity-averaged freezeout hypersurface (S)



- Similar trend with baryon chemical potentials, but absolute values are smaller
- Need more statistics to make strict conclusions
- Need wider range EoS

Introduction

Model

Results

 **Summary and Outlook**

Summary and Outlook

Summary

- Extended the DCCI model to finite baryon number
 - ➡ descriptions of thermalized baryon number
 - ➡ Rapidity Scan!!
- Negative $n_B(\mu_B)$ region appears due to the depositions of anti-quarks
- At LHC energies, high baryon chemical potentials are realized in forward rapidities

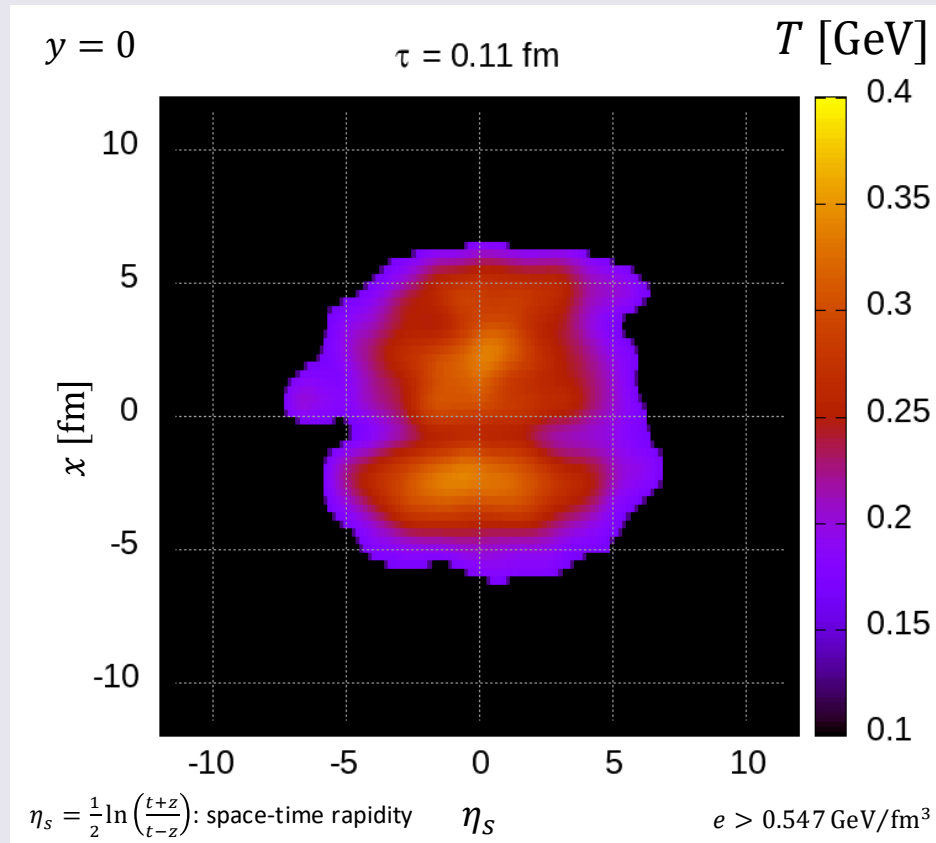
Outlook

- Event averaged analysis, centrality dependence, different initial conditions, *etc.*
- Rapidity dependent analysis (strangeness enhancement, *etc.*)
- Study of QCD phase diagram with rapidity scan (as a complementary way to BES)

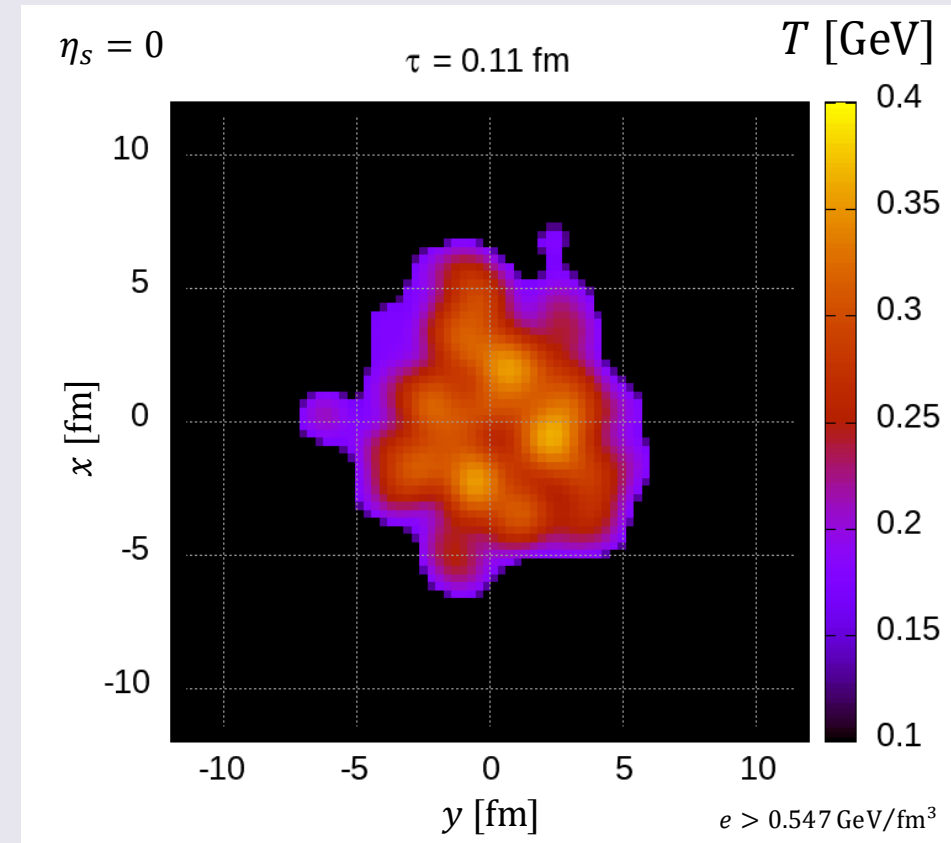
Backups

Space-time evolution of core

Temperature (longitudinal profile)



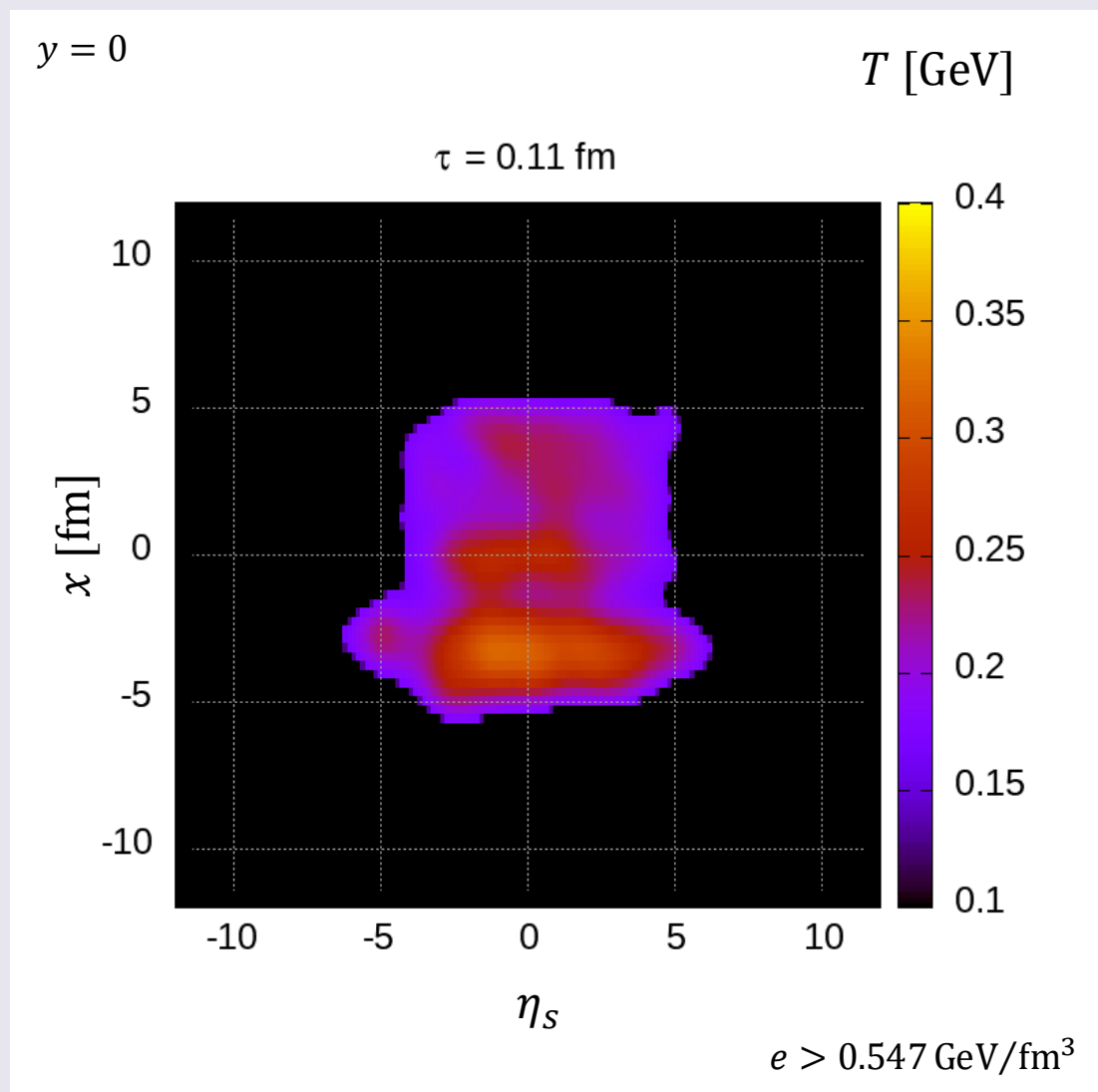
Temperature (transverse profile)



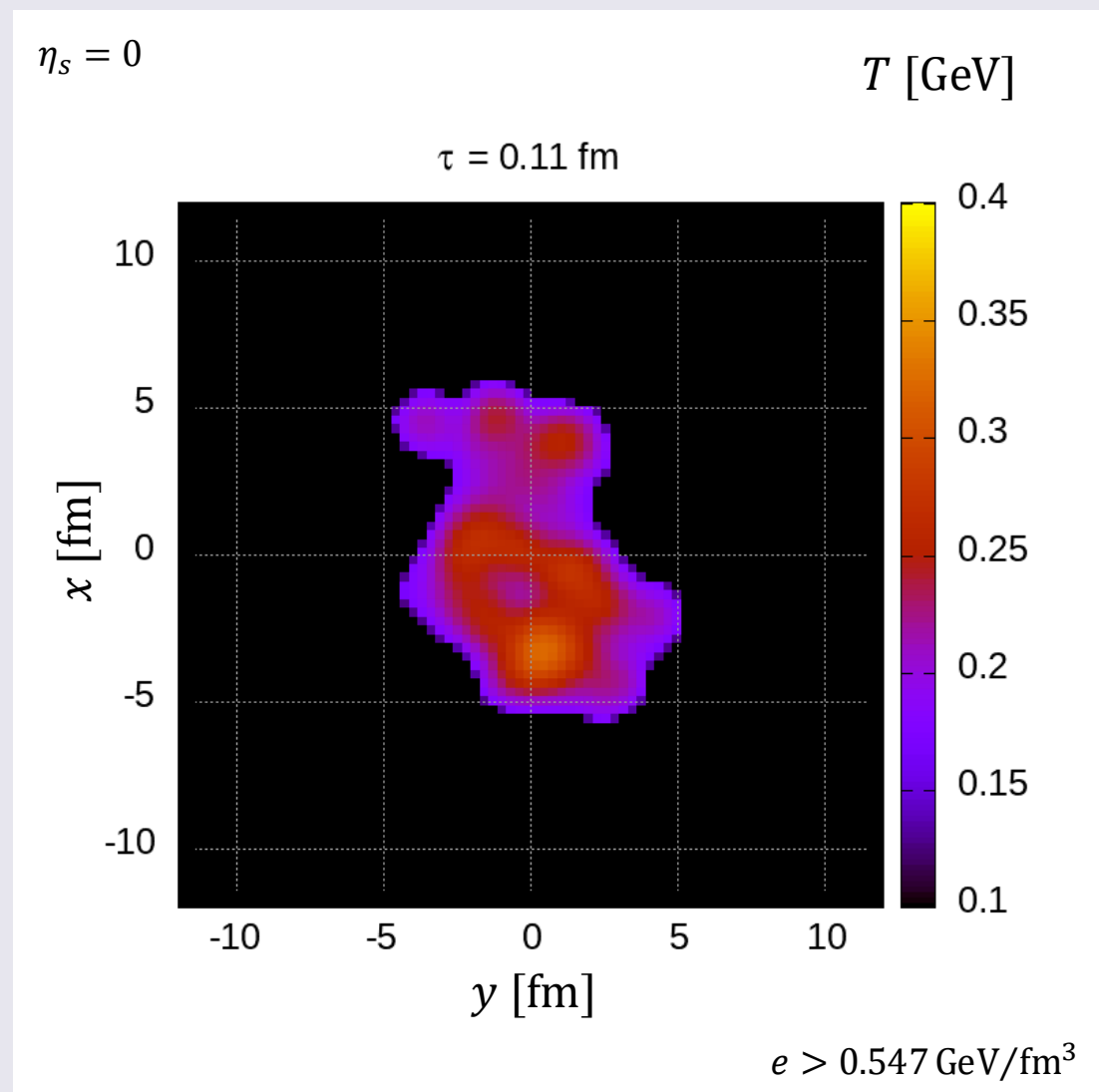
- Gradual formation of the core (QGP fluid) through the energy-momentum source term
- Alongside the fluid formation, the core cools down due to the hydrodynamic evolution

Space-time evolution of core

Temperature (longitudinal profile)

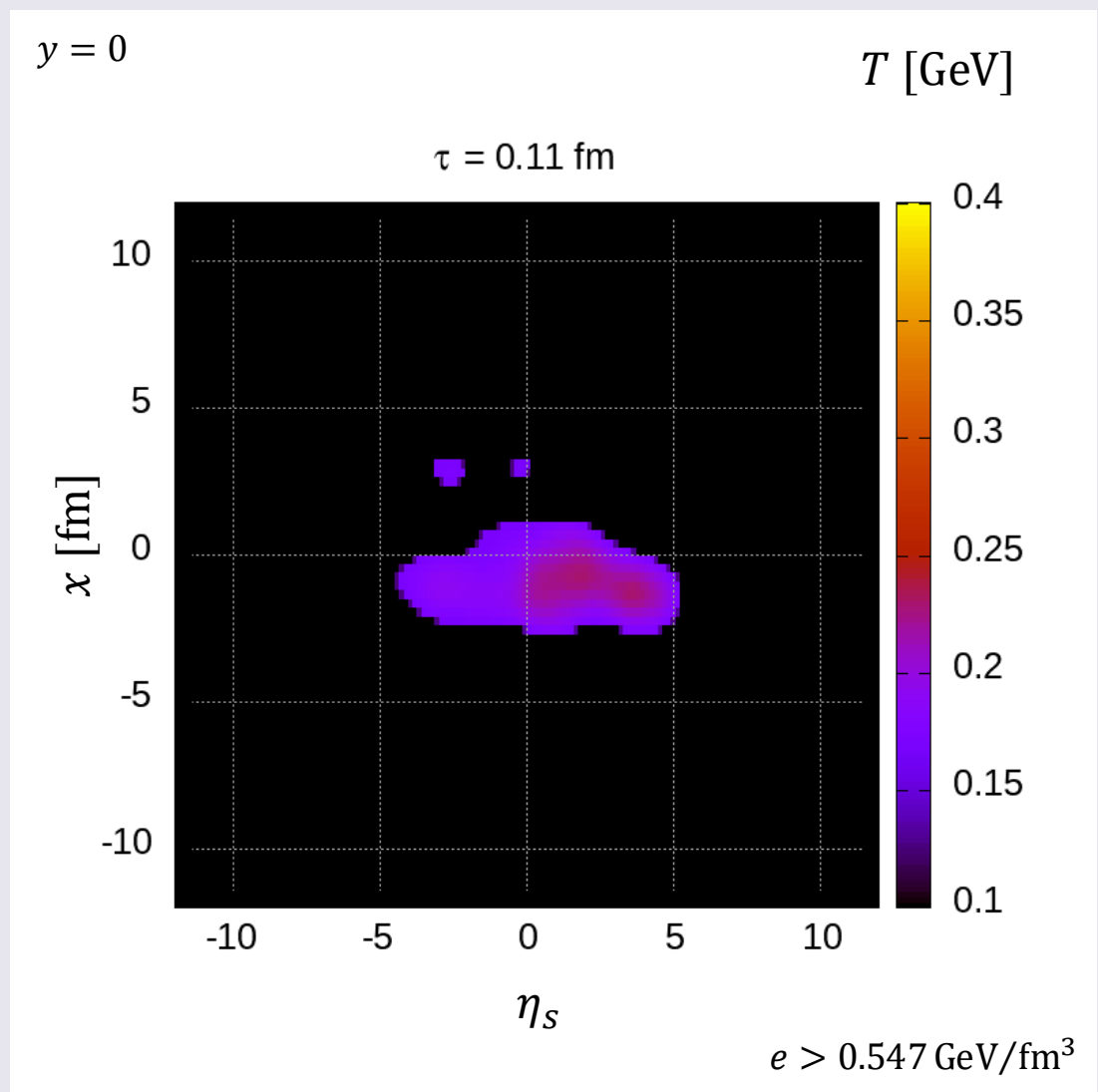


Temperature (transverse profile)

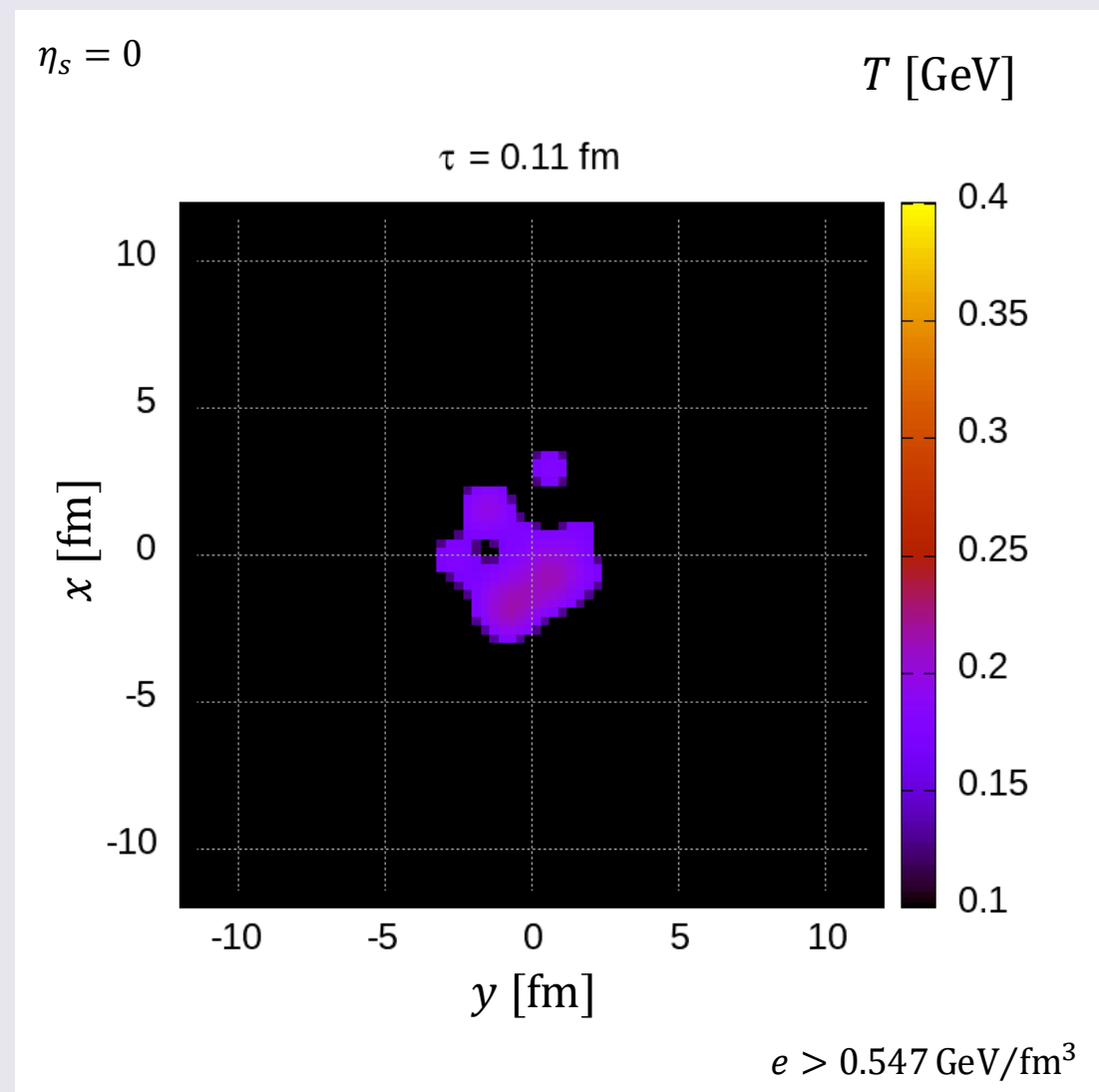


Space-time evolution of core

Temperature (longitudinal profile)

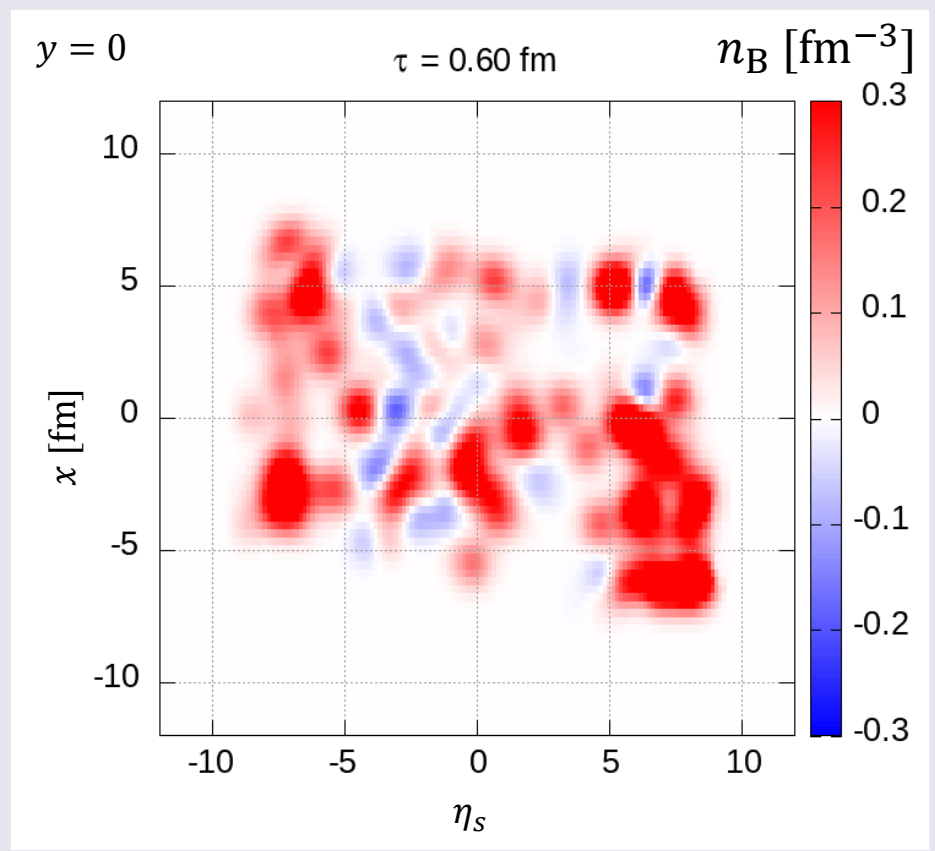


Temperature (transverse profile)

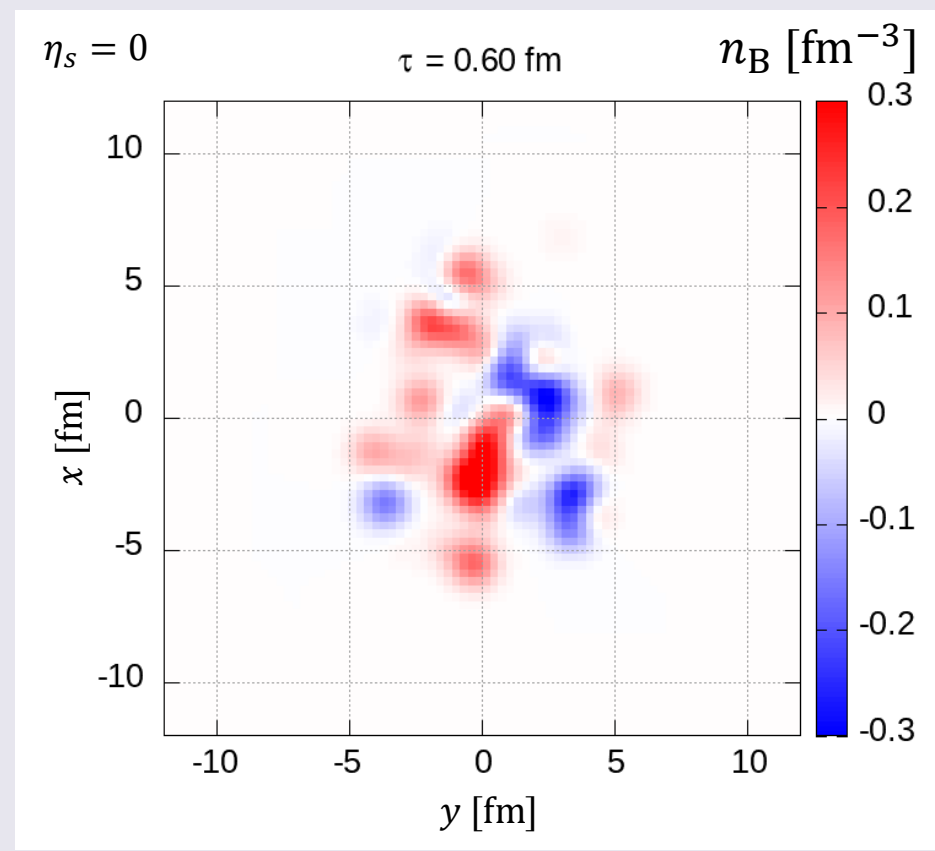


Space-time evolution of core

Baryon number density (longitudinal profile)



Baryon number density (transverse profile)



- Large baryon number density is realized in forward rapidities $5 \lesssim |\eta_s| \lesssim 10$

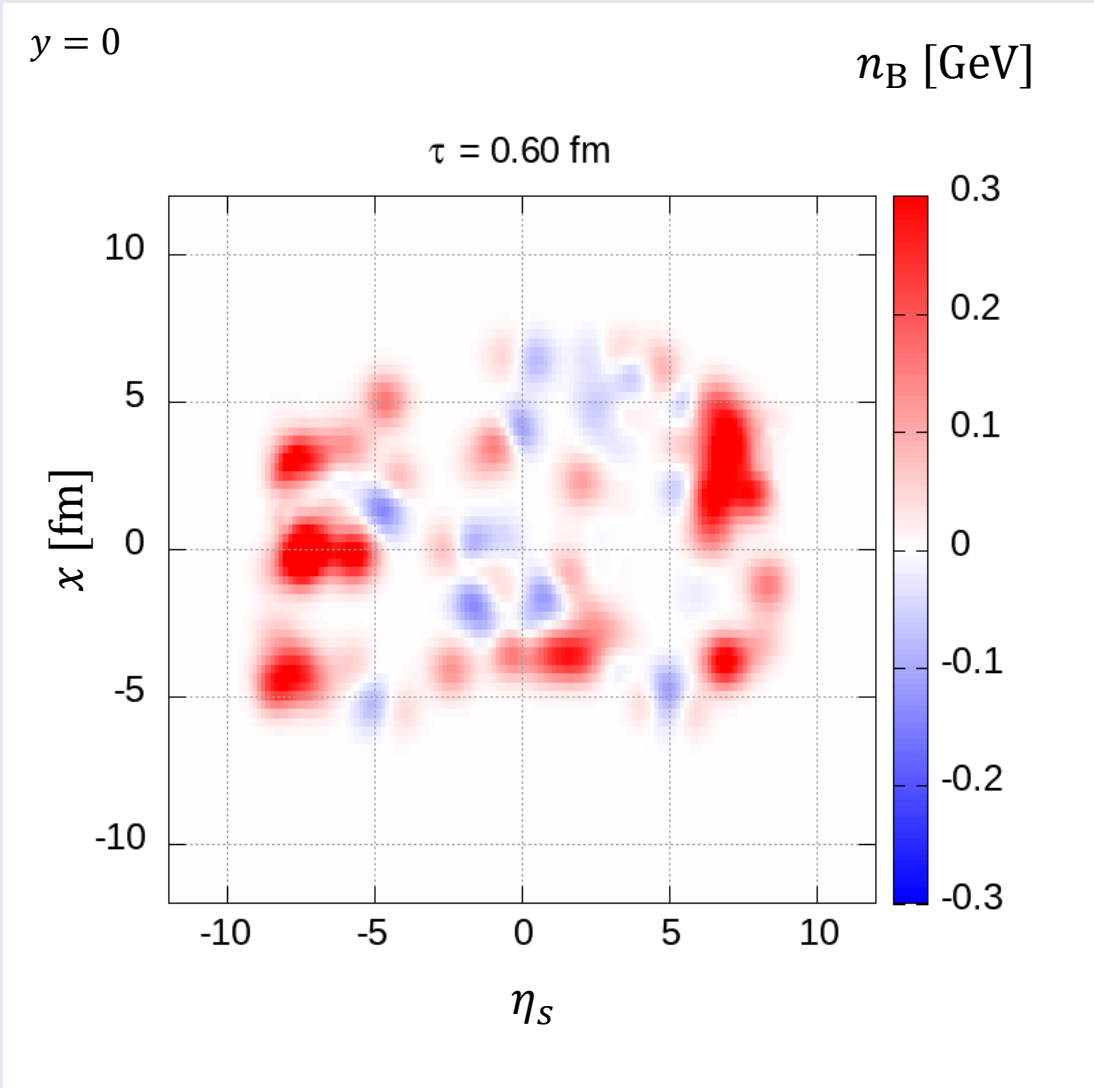
cf.) $y_{\text{beam}}(\sqrt{s_{\text{NN}}} = 2.76 \text{ TeV}) \approx 8$

- Large fluctuations of baryon number density even in midrapidity

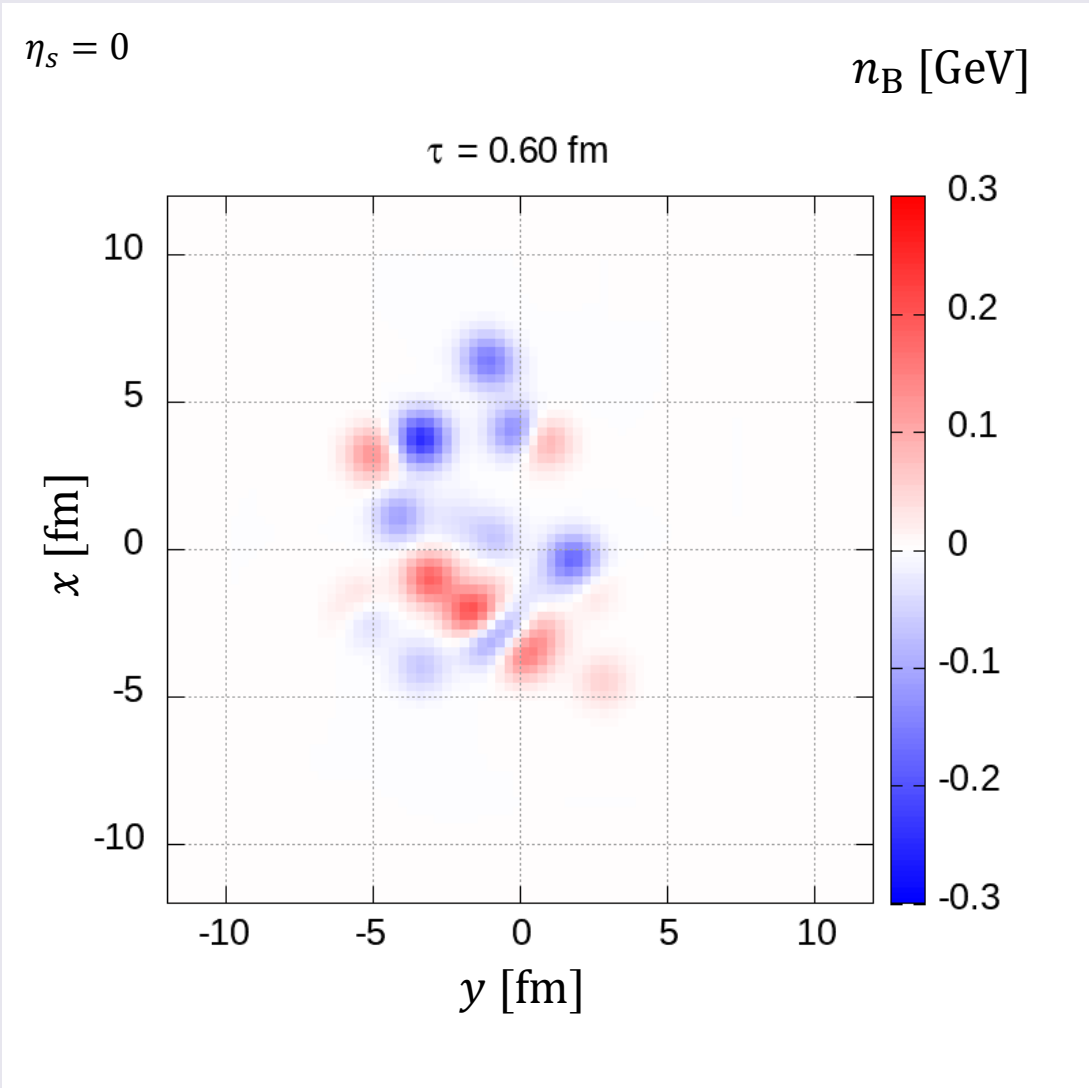
➡ Negative n_B region appears

Space-time evolution of core

Baryon number density (longitudinal profile)

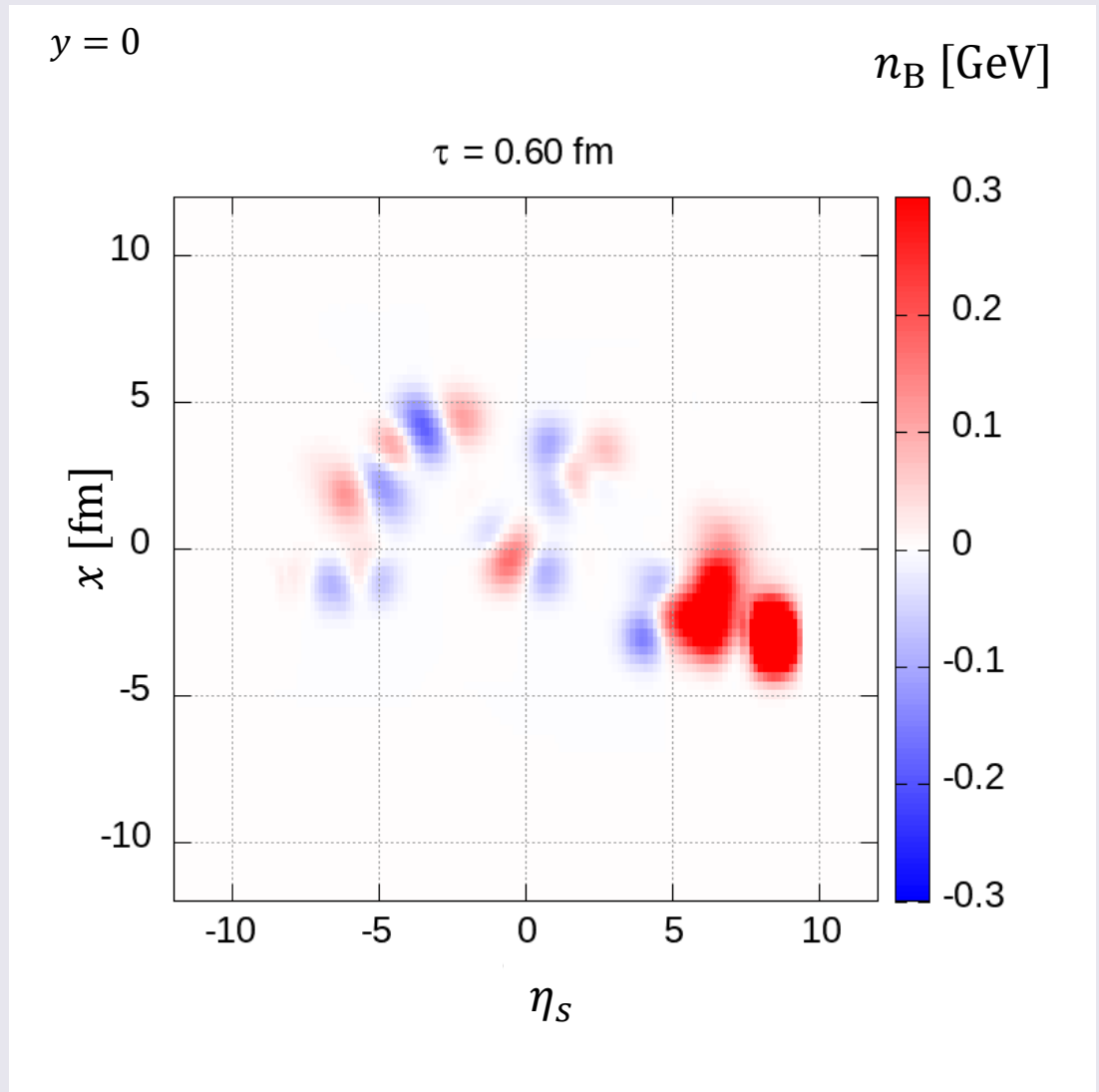


Baryon number density (transverse profile)

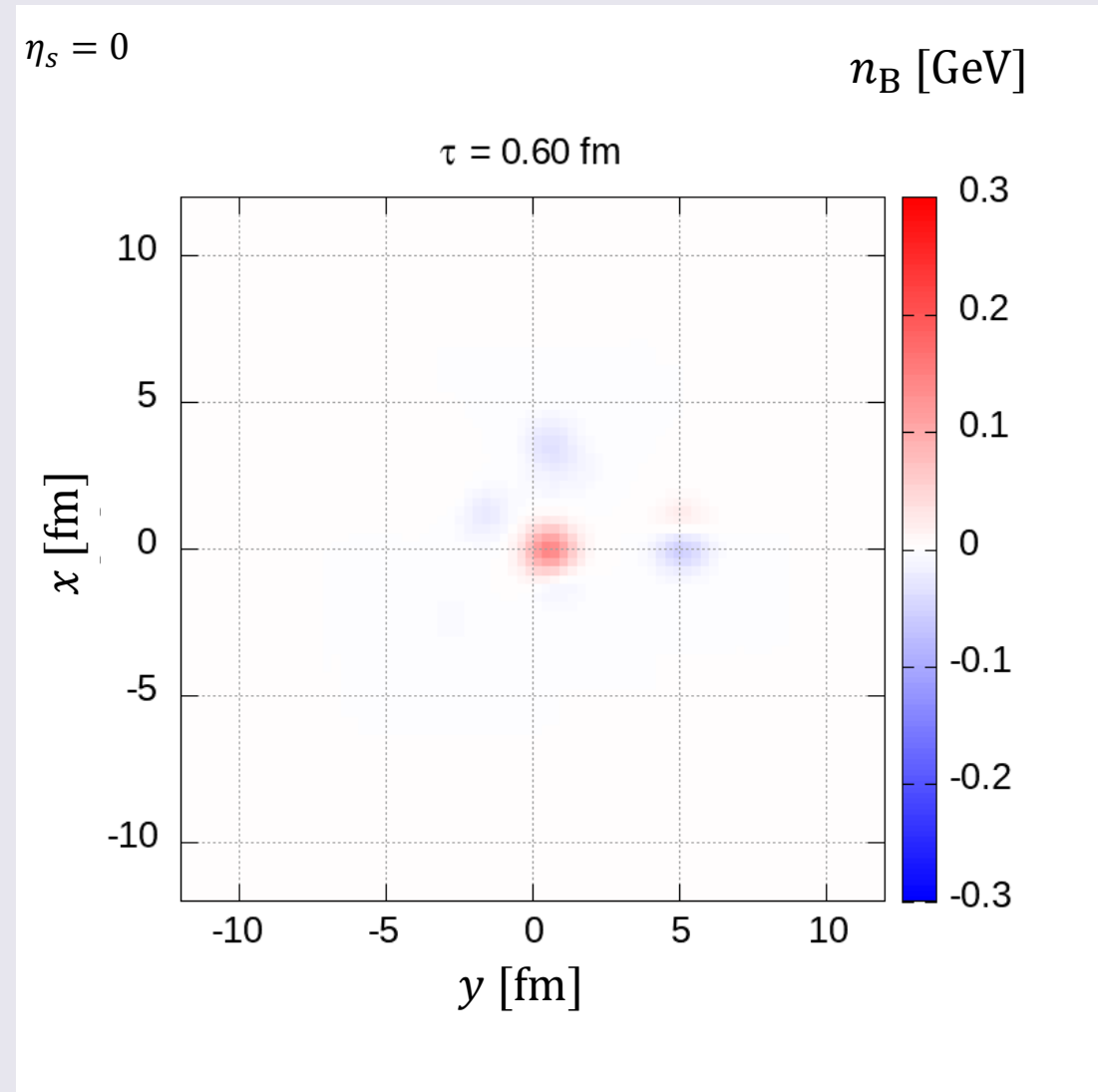


Space-time evolution of core

Baryon number density (longitudinal profile)

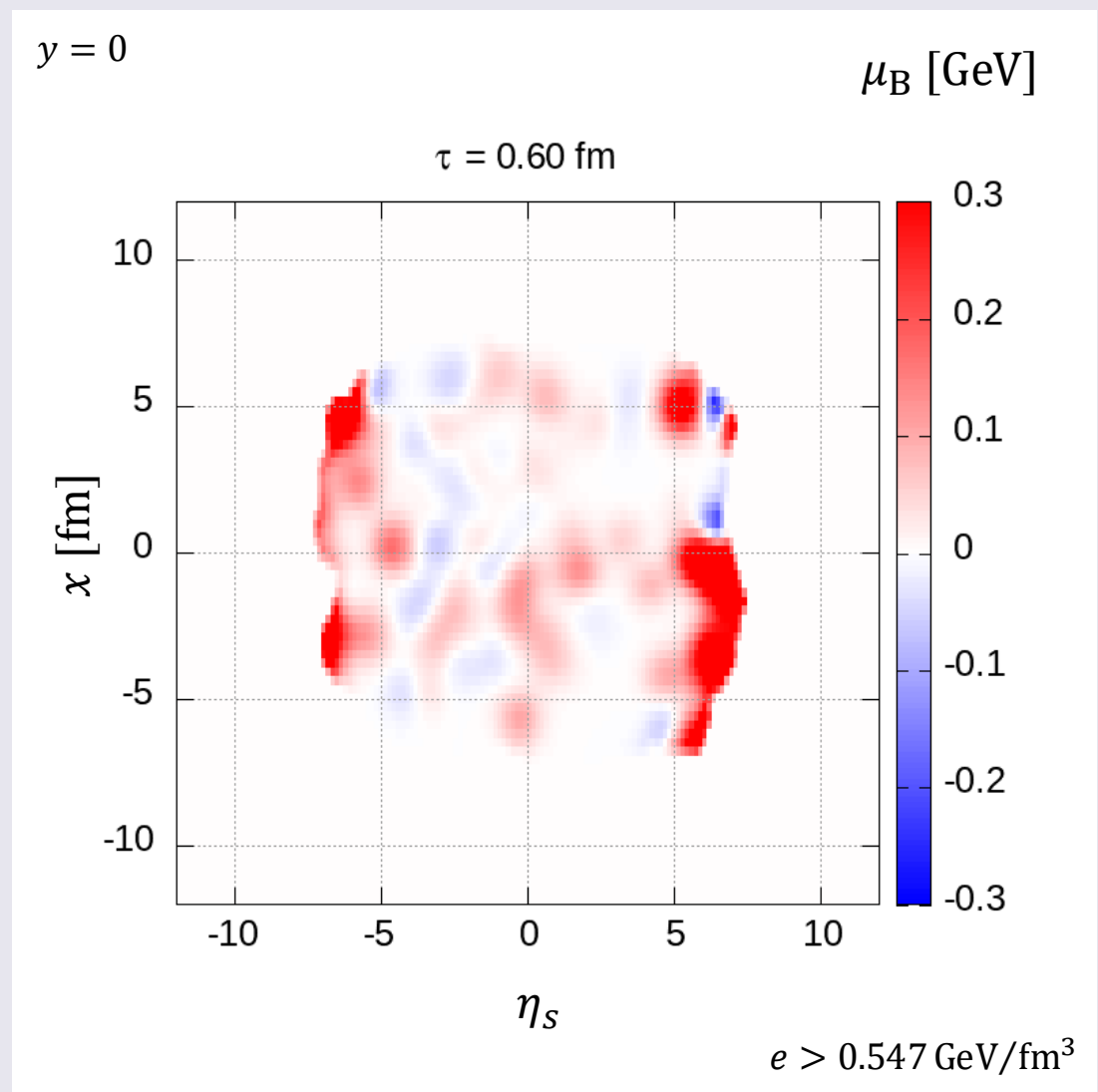


Baryon number density (transverse profile)

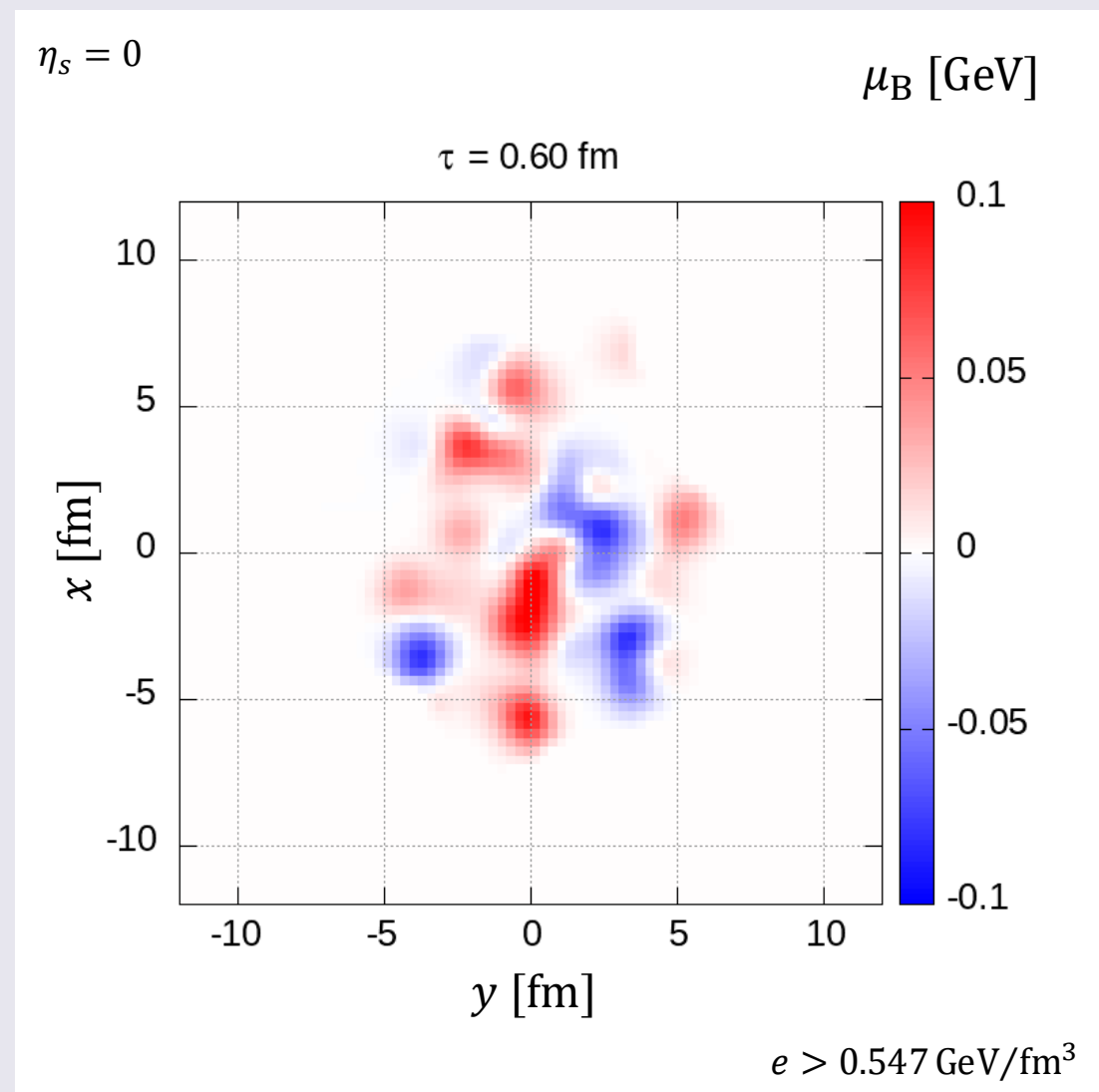


Space-time evolution of core

Baryon chemical potential (longitudinal profile)

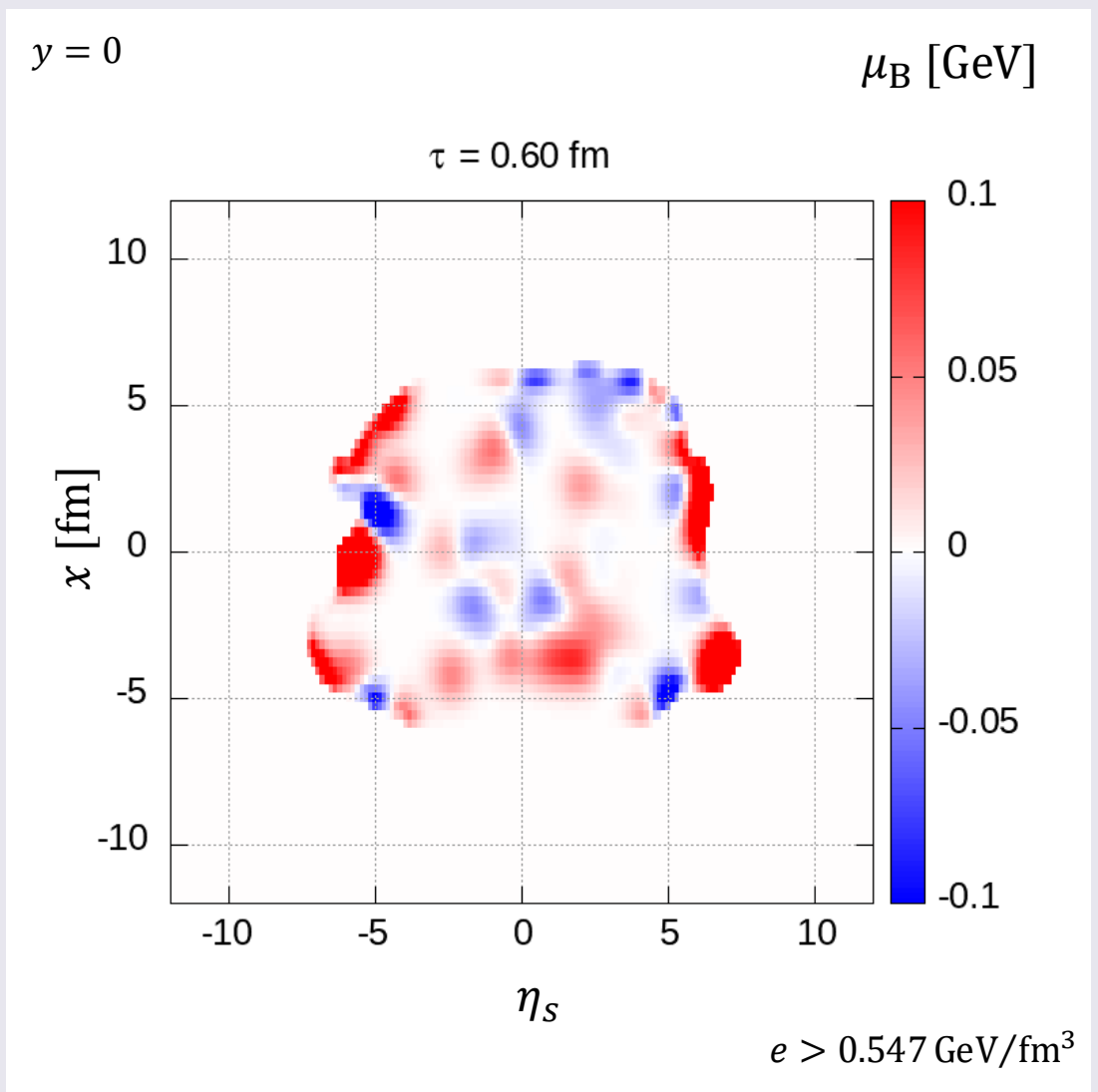


Baryon chemical potential (transverse profile)

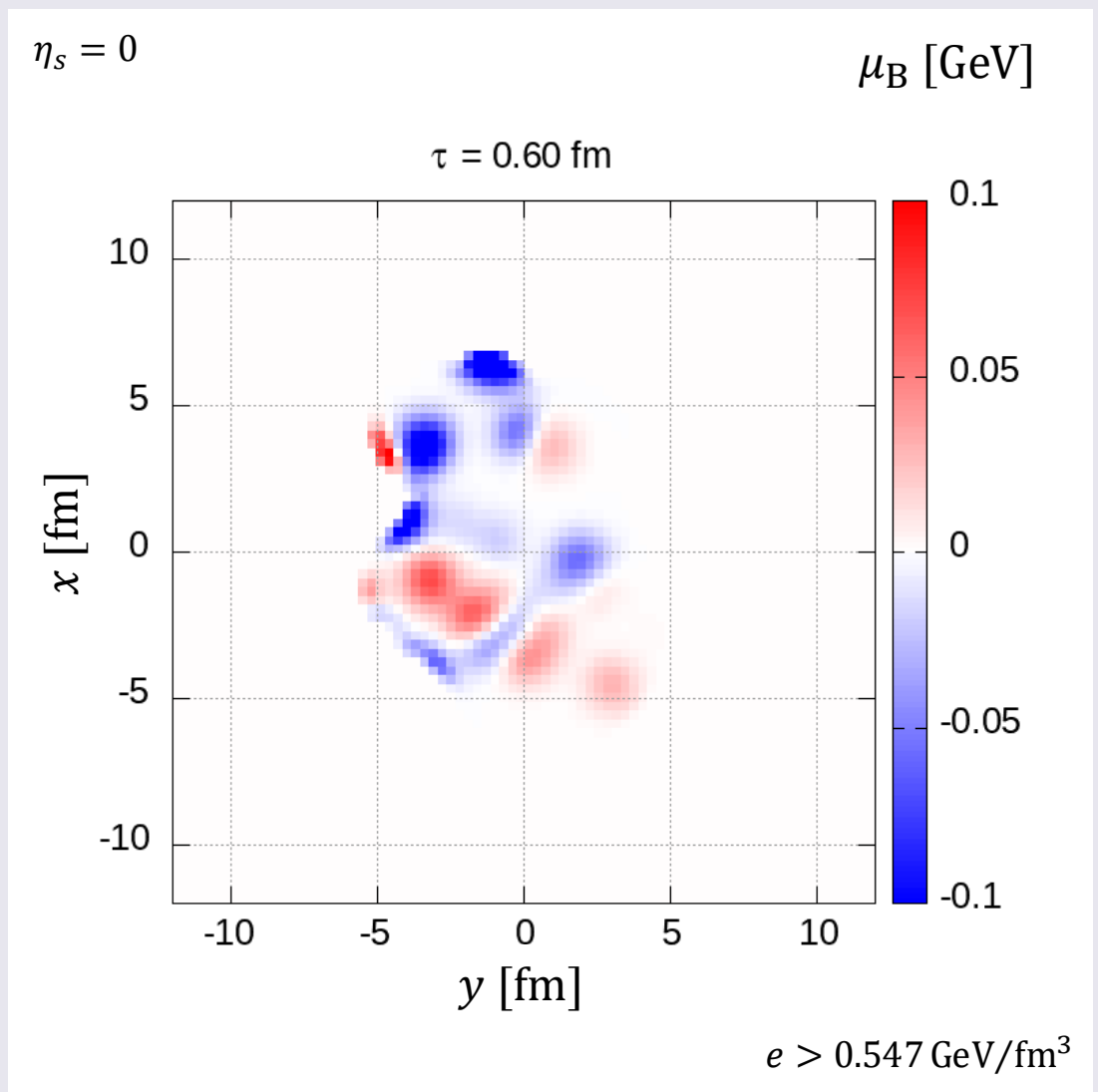


Space-time evolution of core

Baryon chemical potential (longitudinal profile)

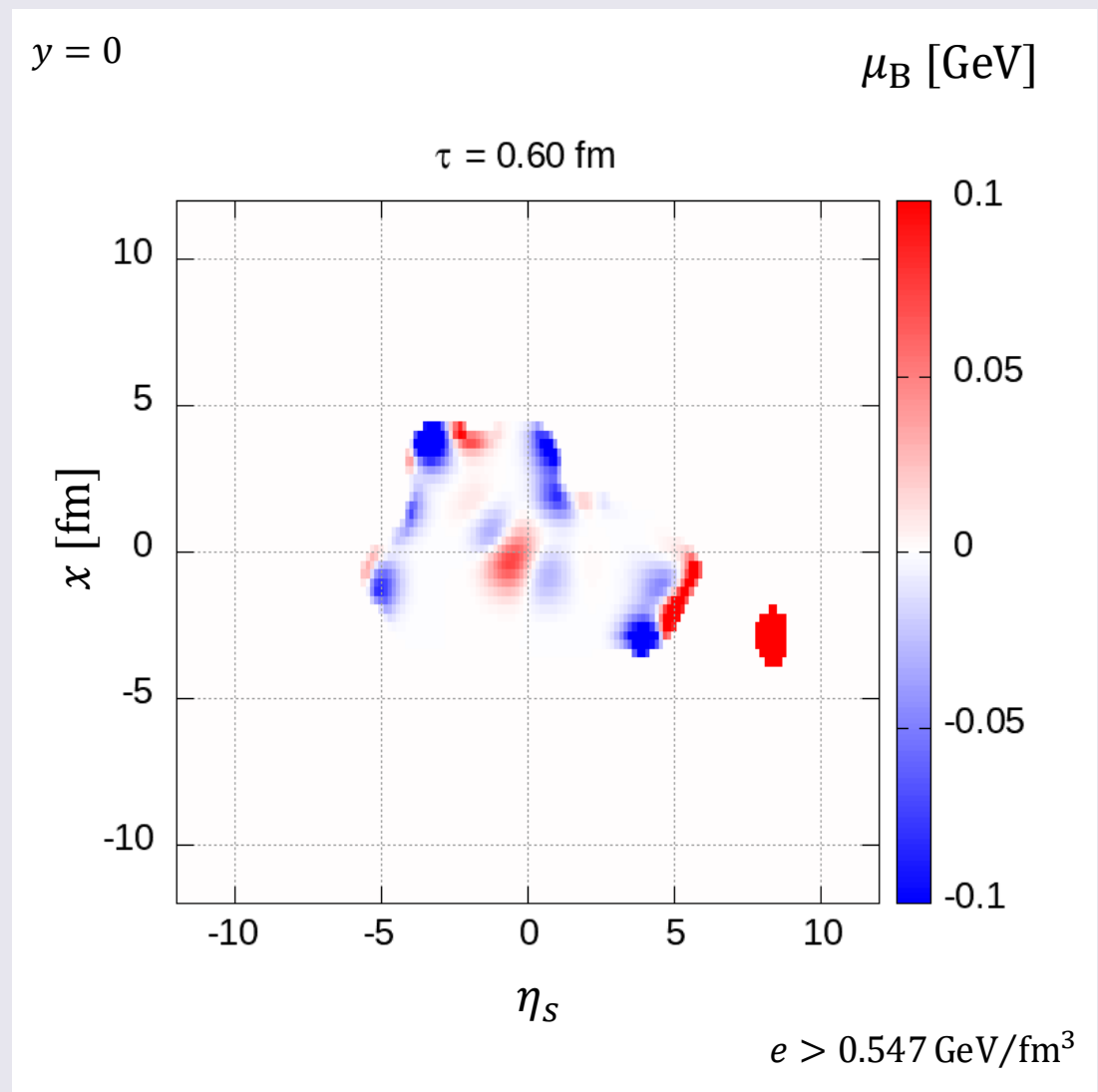


Baryon chemical potential (transverse profile)

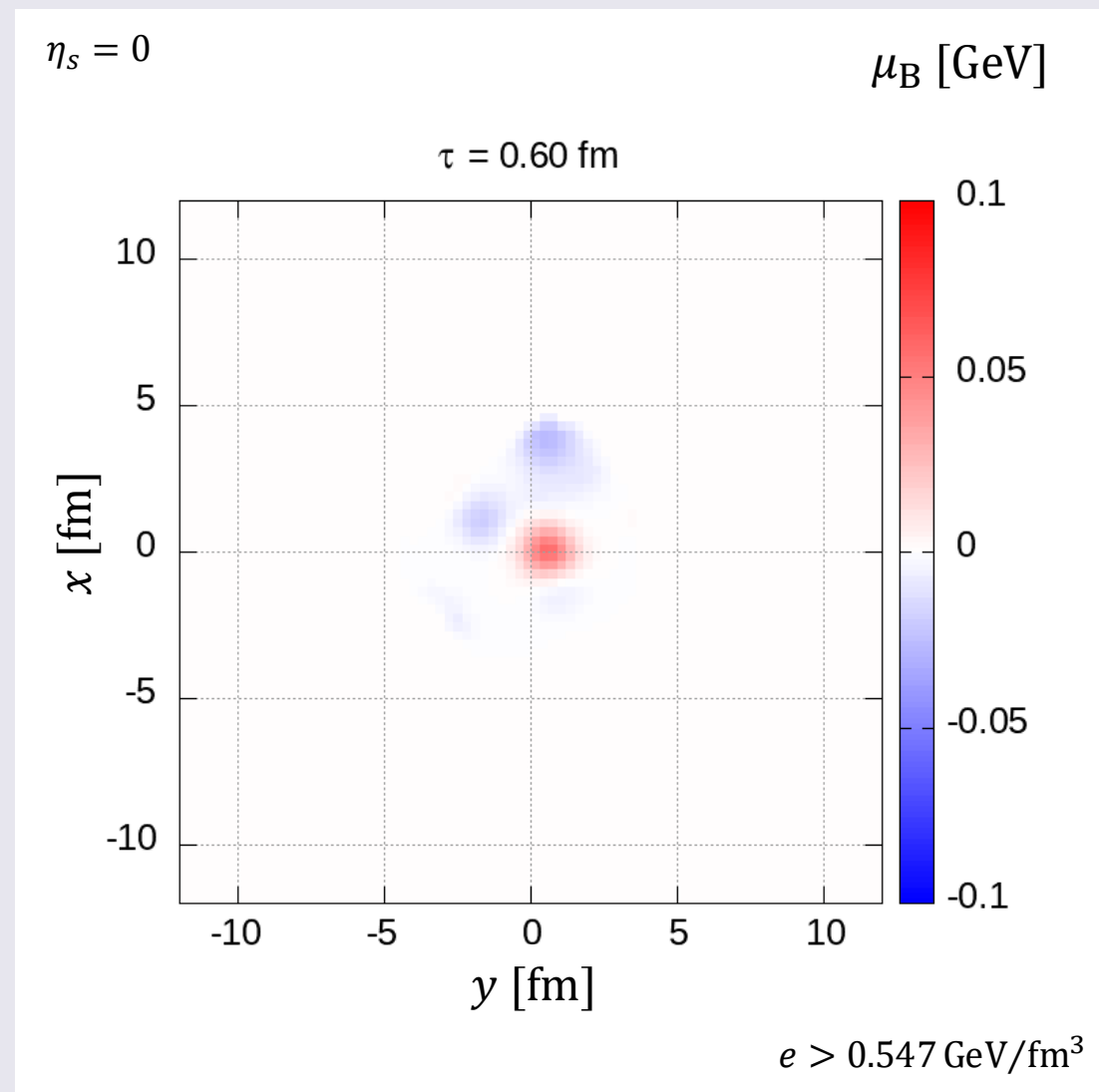


Space-time evolution of core

Baryon chemical potential (longitudinal profile)



Baryon chemical potential (transverse profile)

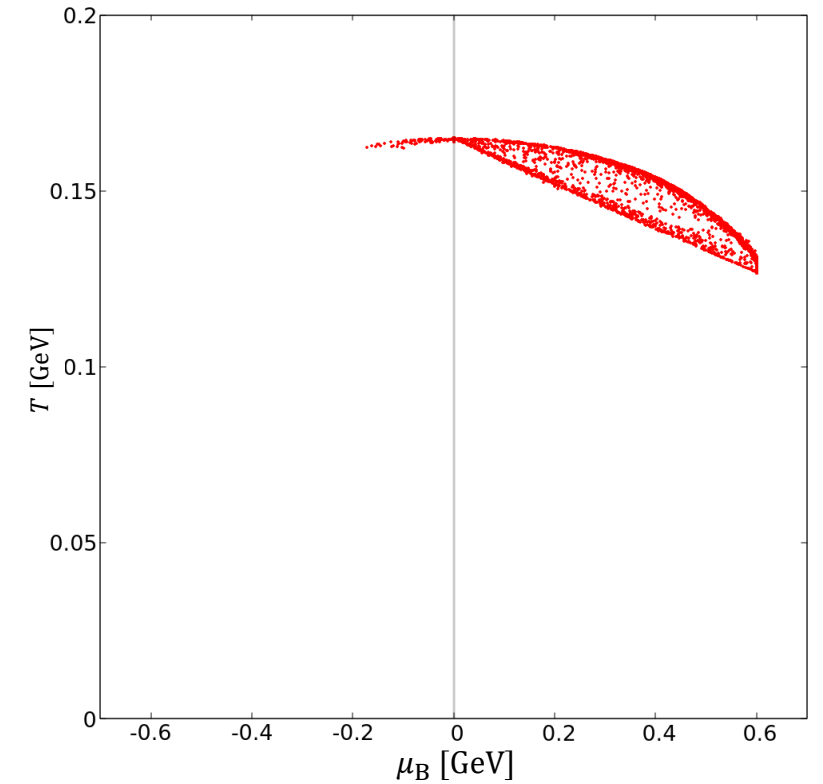
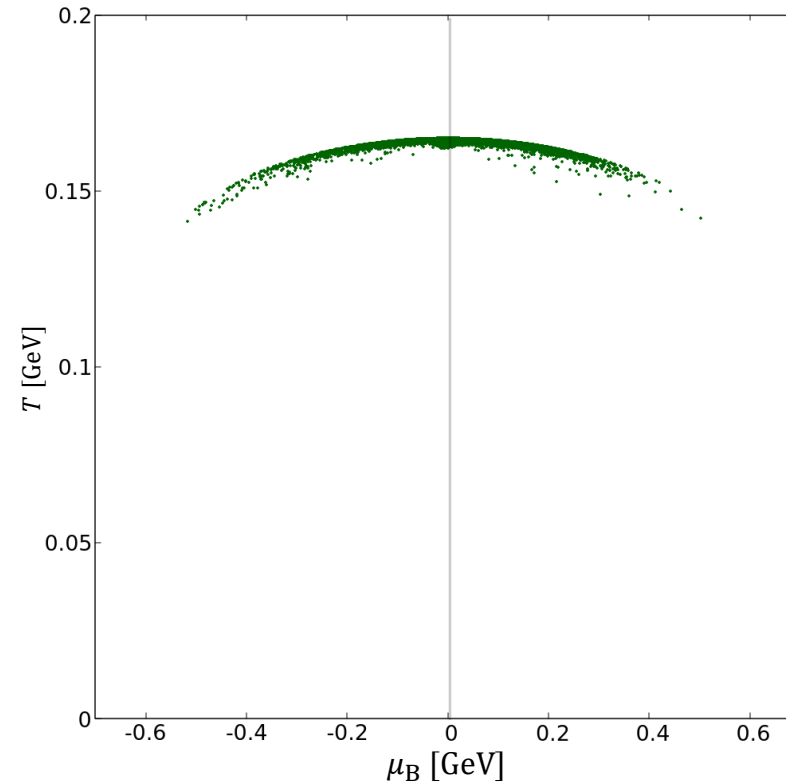
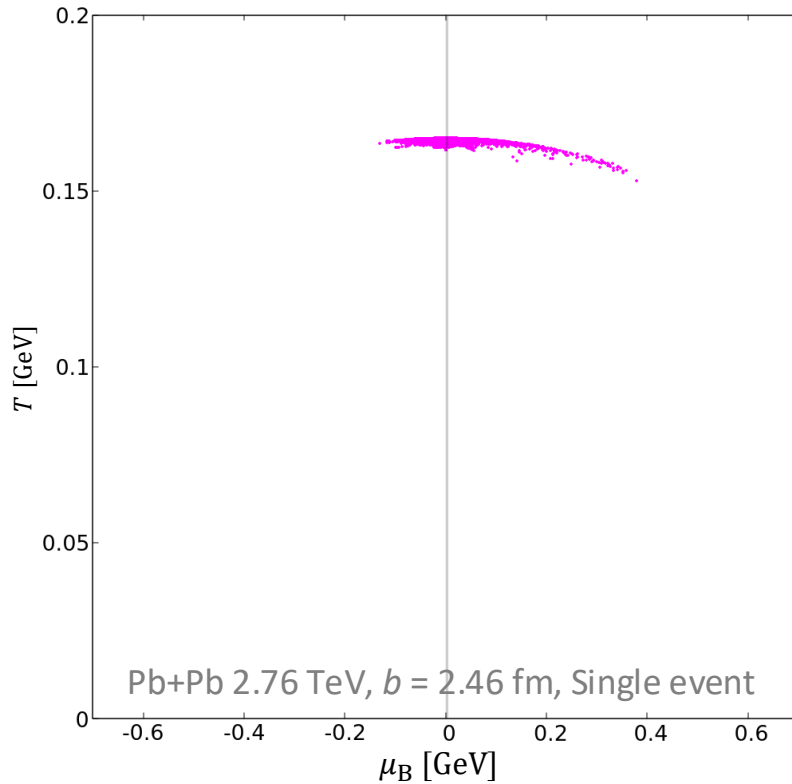


Rapidity dependence of freezeout hypersurface

$$-1 \leq \eta_s \leq 1$$

$$3 \leq \eta_s \leq 5$$

$$7 \leq \eta_s \leq 9$$



- Some hypersurface element has negative baryon chemical potentials
- Significantly large baryon chemical potentials in forward rapidities

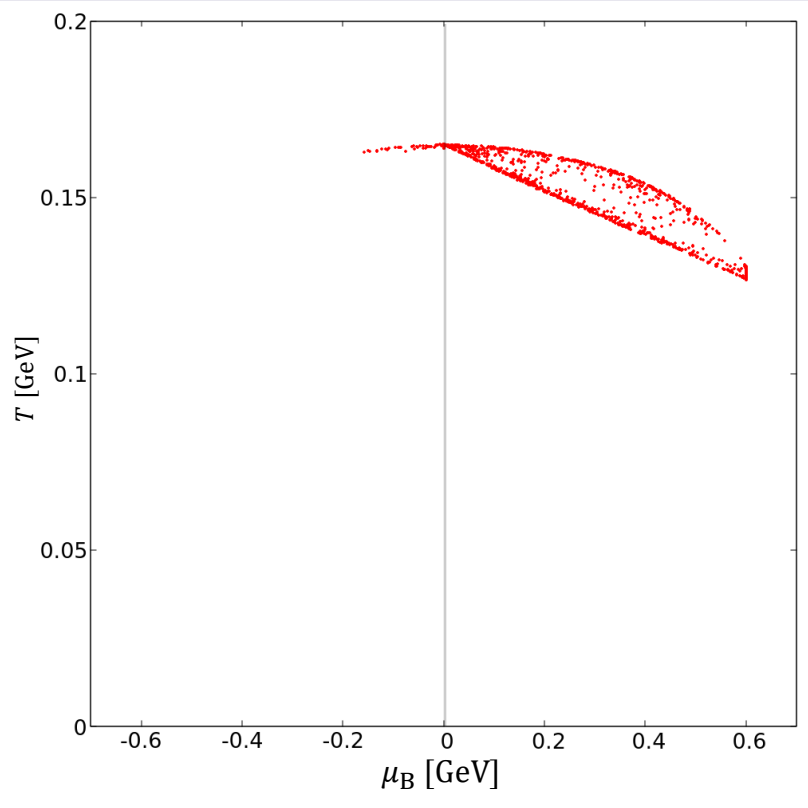
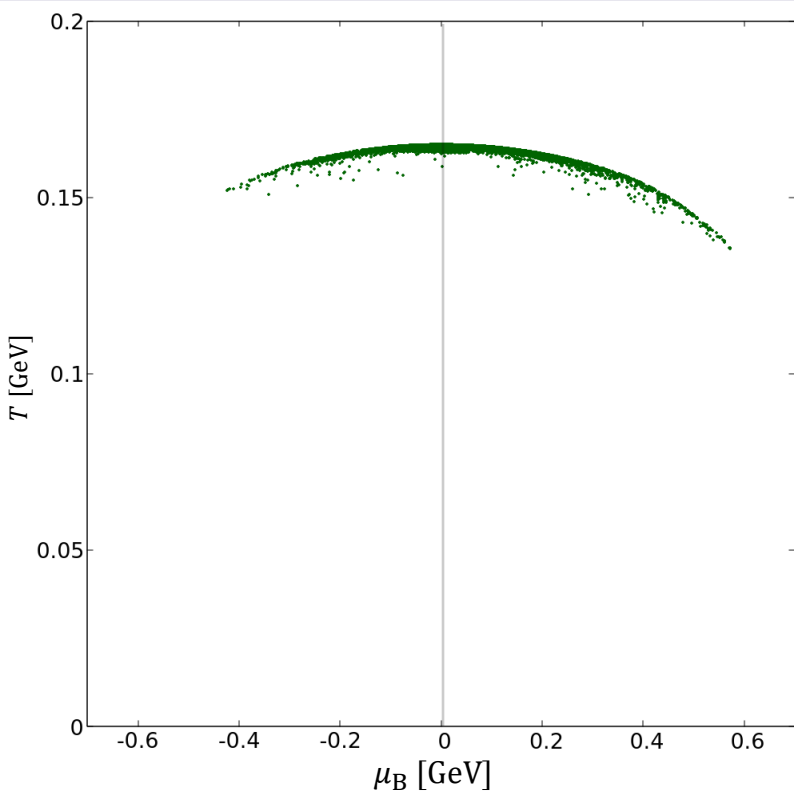
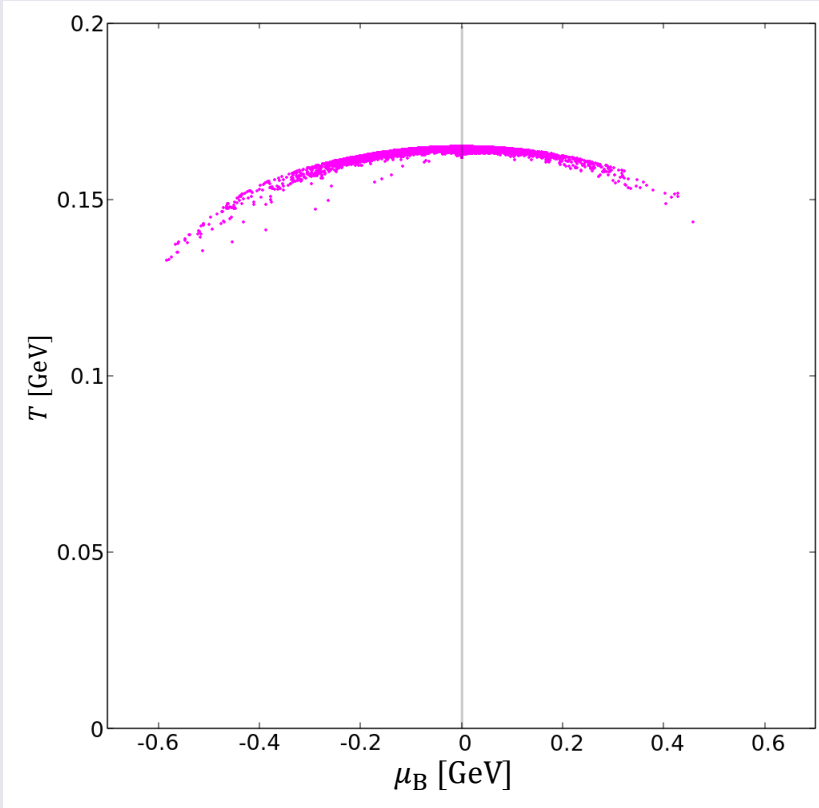
Rapidity dependence of freezeout hypersurface

Pb+Pb 2.76 TeV, $b = 6.12$ fm, Single event

$-1 \leq \eta_s \leq 1$

$3 \leq \eta_s \leq 5$

$7 \leq \eta_s \leq 9$



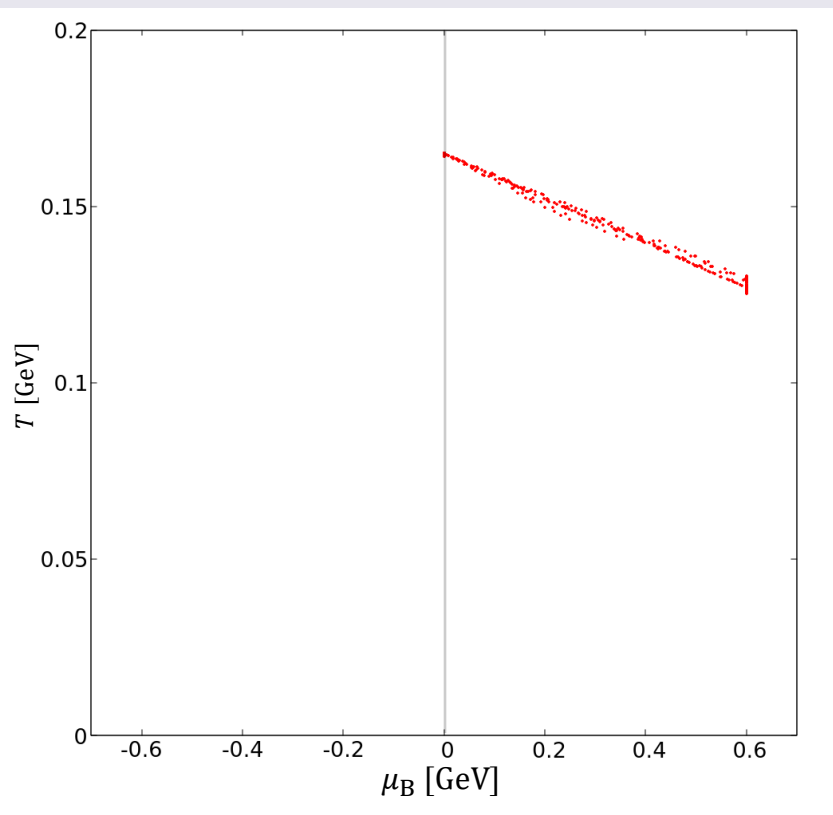
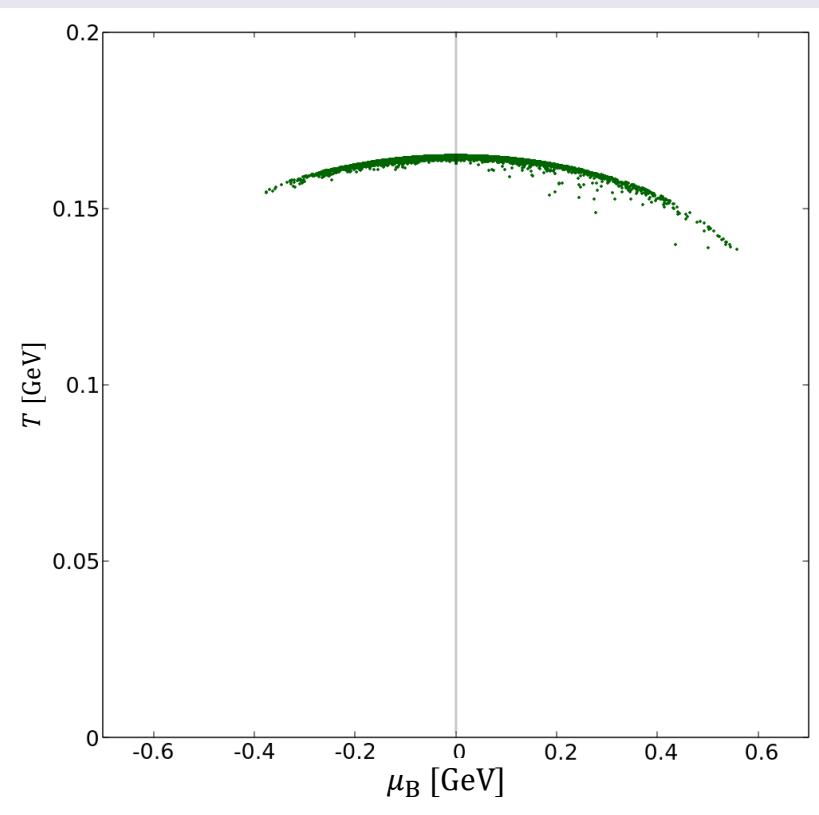
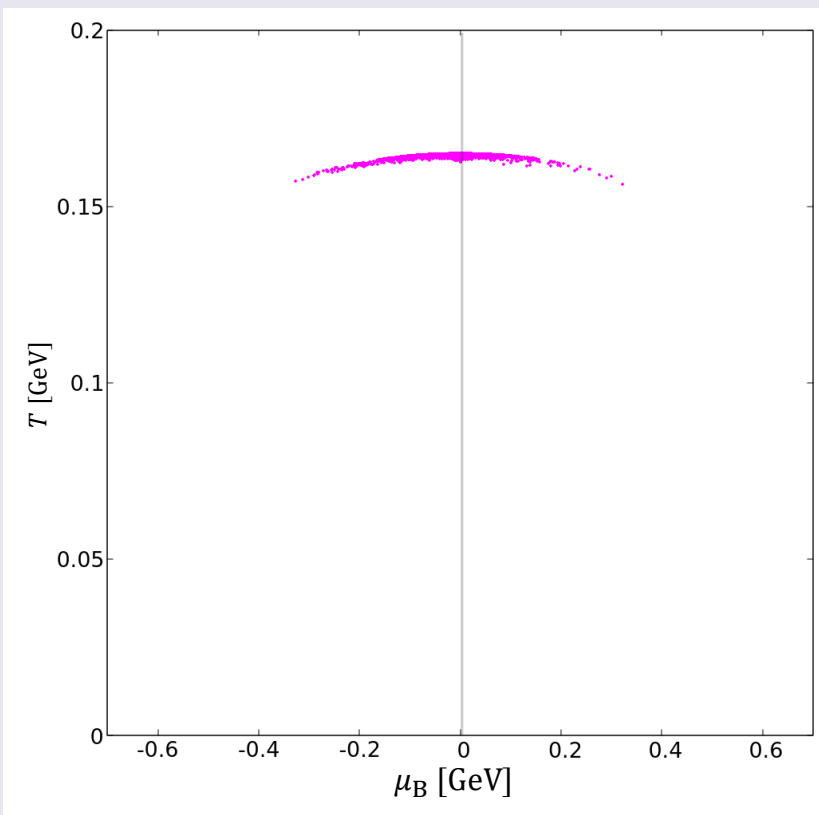
Rapidity dependence of freezeout hypersurface

Pb+Pb 2.76 TeV, $b = 10.1$ fm, Single event

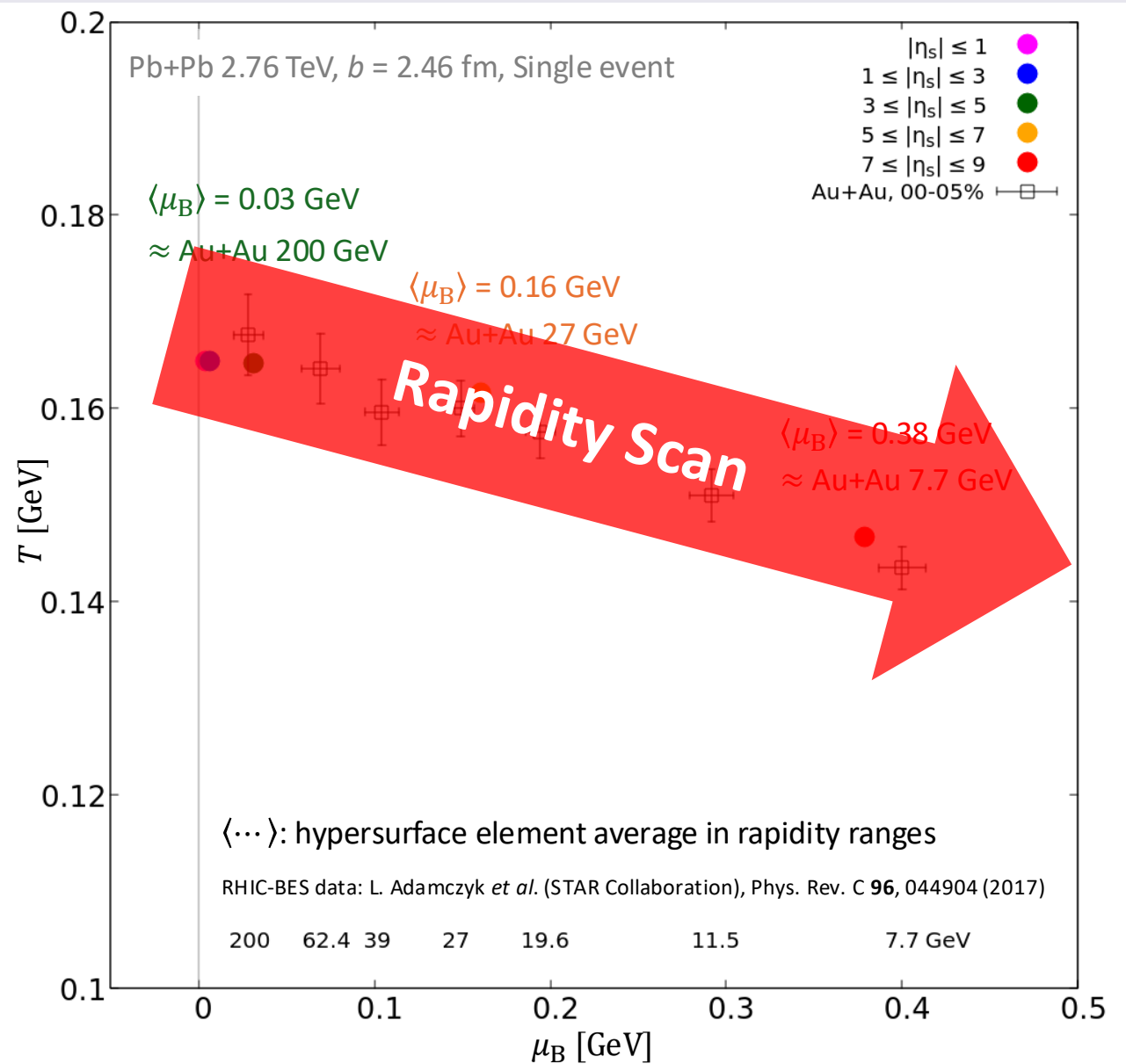
$-1 \leq \eta_s \leq 1$

$3 \leq \eta_s \leq 5$

$7 \leq \eta_s \leq 9$



Rapidity-averaged freezeout hypersurface

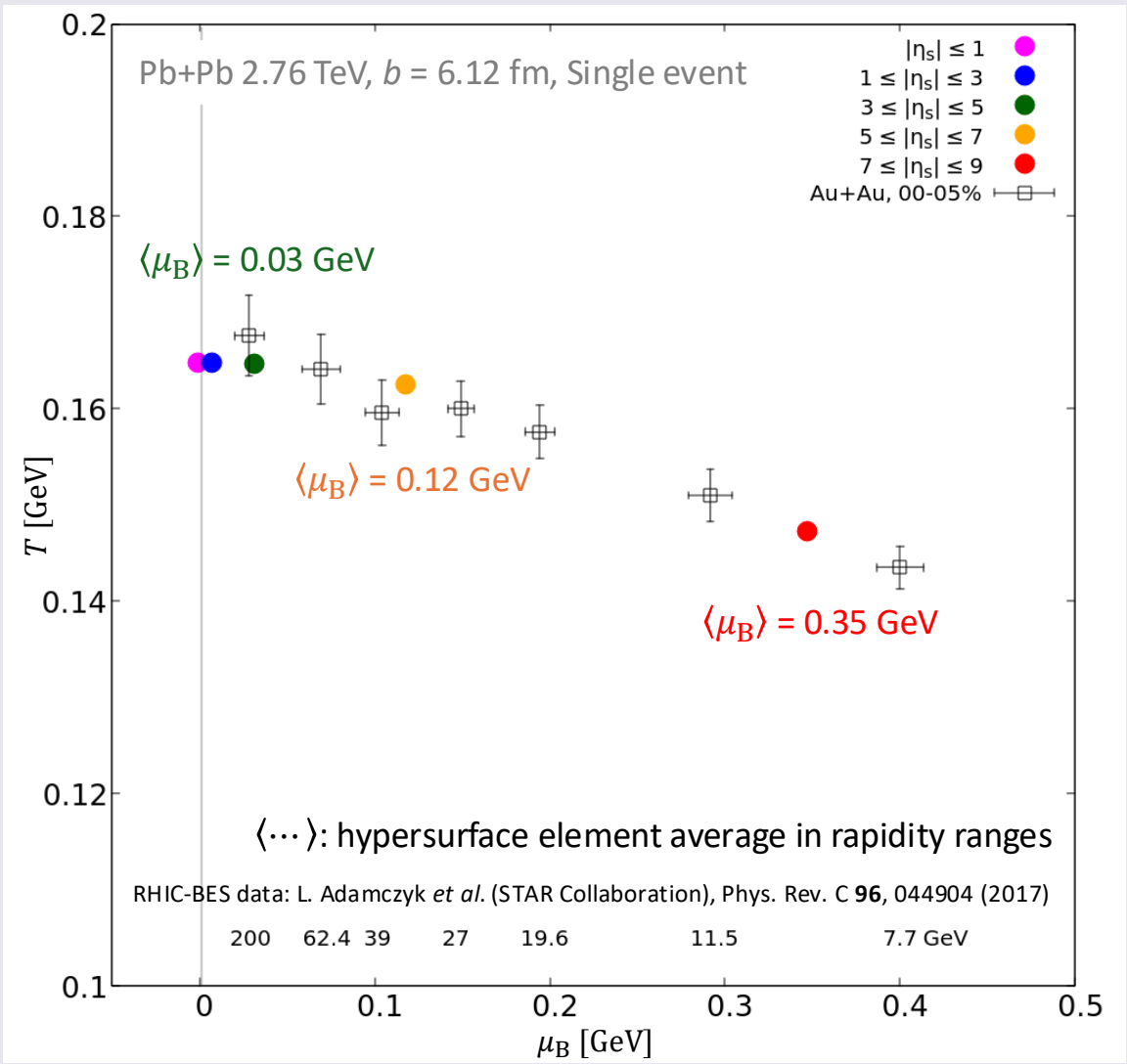


- Almost zero baryon chemical potential until $|\eta_s| \leq 5$
 - ➔ \approx Au+Au 200 GeV
- Averaged-hypersurface in rapidity range $5 \leq |\eta_s| \leq 7$ exceeds $\mu_B = 100$ MeV
 - ➔ \approx **Au+Au 27 GeV**
- Averaged-hypersurface in rapidity range $7 \leq |\eta_s| \leq 9$ exceeds $\mu_B = 300$ MeV
 - ➔ \approx **Au+Au 7.7 GeV**

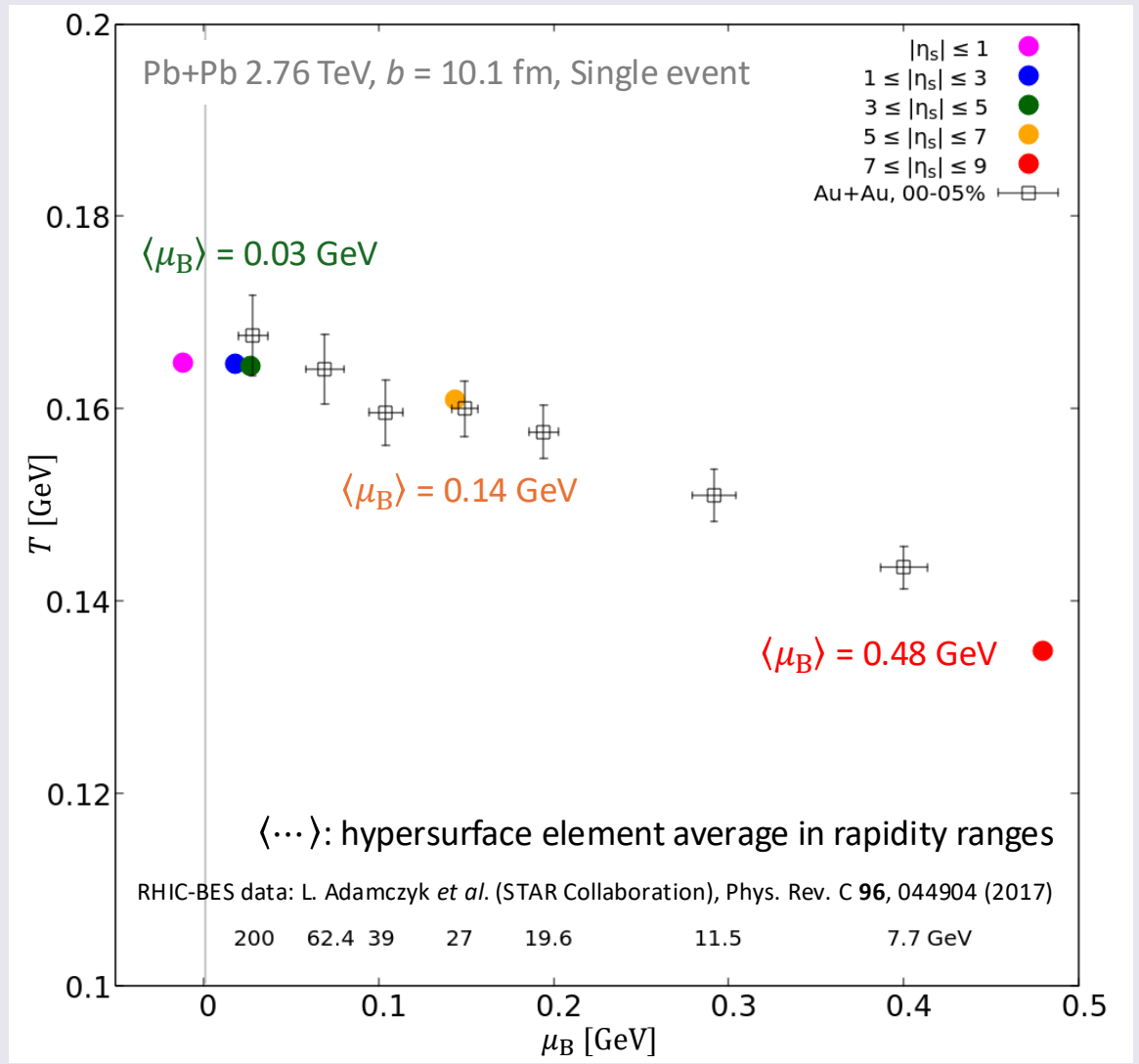
Rapidity scan is a strong tool for exploring the QCD phase diagram!!

Rapidity-averaged freezeout hypersurface

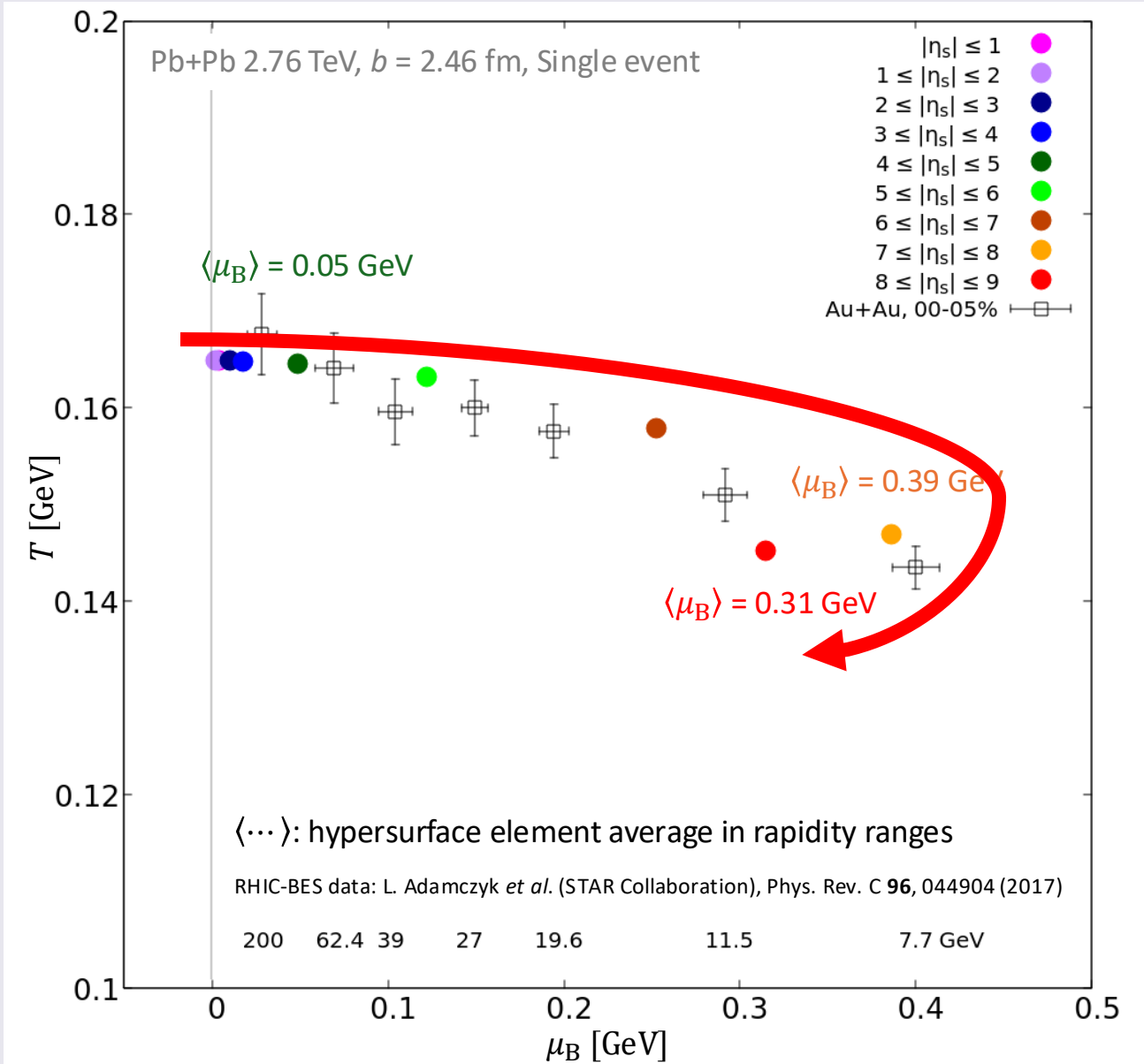
$b = 6.12$ fm



$b = 10.1$ fm



Rapidity-averaged freezeout hypersurface



● μ_B becomes maximum in $7 \leq |\eta_s| \leq 8$

cf.) $y_{\text{beam}}(\sqrt{s_{\text{NN}}} = 2.76 \text{ TeV}) \approx 8$

NEOS-BQS

Taylor expansion using Lattice results (high T)

$$\frac{P}{T^4} = \frac{P_0}{T^4} + \sum_{l,m,n} \frac{x_{l,m,n}^{B,Q,S}}{l,m,n} \left(\frac{\mu_B}{T}\right)^l \left(\frac{\mu_Q}{T}\right)^m \left(\frac{\mu_S}{T}\right)^n$$

Hadron gas (low T)

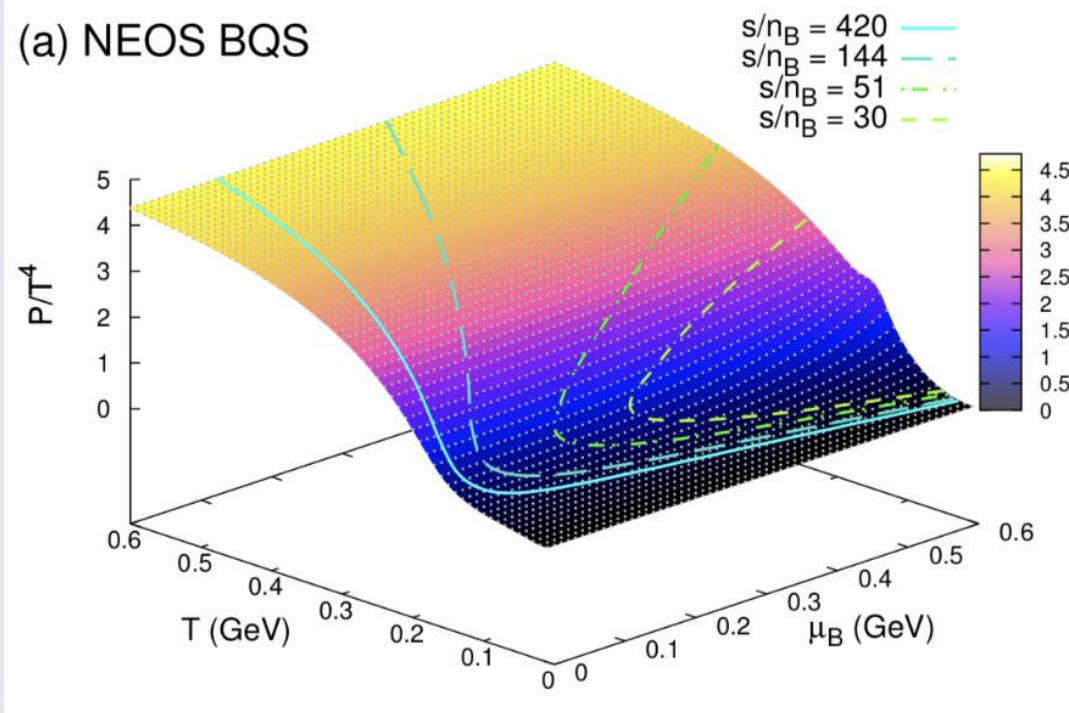
$$P = \pm T \sum_i \int \frac{g_i d^3p}{(2\pi)^3} \ln[1 \pm e^{-(E_i - \mu_i)/T}]$$

$$= \sum_i \sum_k (\mp 1)^{k+1} \frac{1}{k^2} \frac{g_i}{2\pi^2} m_i^2 T^2 e^{k\mu_i/T} K_2\left(\frac{km_i}{T}\right)$$

CONNECT

$$\frac{P}{T^4} = \frac{1}{2} [1 - f(T, \mu_J)] \frac{P_{\text{had}}(T, \mu_J)}{T^4} + \frac{1}{2} [1 + f(T, \mu_J)] \frac{P_{\text{lat}}(T, \mu_J)}{T^4}$$

(a) NEOS BQS



Constraints: $n_Q = 0.4n_B$, $n_S = 0$

$$e(T, \mu_B) = e(0.165 \text{ GeV}, 0) = 0.547 \text{ GeV/fm}^3$$

➡ e_{sw} for core

Hydrodynamic module in DCCI

Energy-momentum conservation

$$\partial_\mu T_{\text{fluid}}^{\mu\nu} = j^\nu$$

$$T_{\text{fluid}}^{\mu\nu} = e u^\mu u^\nu - p \Delta^{\mu\nu} \quad \leftarrow \text{ideal hydro}$$

$$j^\nu = - \sum_i \frac{dp_i^\nu(t)}{dt} G(\mathbf{x} - \mathbf{x}_i(t))$$

Baryon number conservation

$$\partial_\mu N_{\text{fluid}}^\mu = \rho$$

$$N_{\text{fluid}}^\mu = n_B u^\mu \quad \leftarrow \text{ideal hydro}$$

$$\rho = - \sum_{i_{\text{dead}}} \frac{dB_{i_{\text{dead}}}}{dt} G(\mathbf{x} - \mathbf{x}_{i_{\text{dead}}}(t))$$

$$G_{\text{Milne}} = \frac{1}{\sqrt{2\pi\sigma_\eta^2\tau^2}} \exp\left(-\frac{(\eta_{s,\text{parton}} - \eta_{s,i})^2}{2\sigma_\eta^2}\right) \times \frac{1}{2\pi\sigma_{xy}^2} \exp\left(-\frac{(x_{\text{parton}} - x_i)^2 + (y_{\text{parton}} - y_i)^2}{2\sigma_{xy}^2}\right)$$

Default: $\sigma_\eta = 0.5$, $\sigma_{xy} = 0.6$ fm

RHIC-BES data

L. Adamczyk *et al.* (STAR Collaboration), Phys. Rev. C **96**, 044904 (2017)

